ACADEMIC PRESS

Available online at www.sciencedirect.com

SCIENCE DIRECT®

DEVELOPMENTAL BIOLOGY

Developmental Biology 260 (2003) 226–244

www.elsevier.com/locate/ydbio

ff1b is required for the development of steroidogenic component of the zebrafish interrenal organ

Chou Chai,[a] Yi-wen Liu,[a,b] and Woon-Khiong Chan[a,b,*]

[a] *Institute of Molecular Agrobiology, 1 Research Link, Singapore 117604*

[b] *Department of Biological Sciences, 14, Science Drive 4, National University of Singapore, Singapore 119260*

Received for publication 20 November 2002, revised 31 March 2003, accepted 31 March 2003

Abstract

The zebrafish *ftz-f1* gene, *ff1b*, is activated in two cell clusters lateral to the midline in the trunk during late embryogenesis. These cell clusters coalesce to form a discrete organ at around 30 hpf, which then begins to acquire a steroidogenic identity as evidenced by the expression of the steroidogenic enzyme genes, *cyp11a* and *3β-hsd*. The migration of the cell clusters to the midline is impaired in zebrafish midline signaling mutants. Knockdown of Ff1b activity by antisense *ff1b* morpholino oligonucleotide (ff1bMO) leads to phenotypes that are consistent with impaired osmoregulation. Injection of ff1bMO was also shown to downregulate the expression of *cyp11a* and *3β-hsd*. Histological comparison of wild-type and *ff1b* morphants at various embryonic and juvenile stages revealed the absence of interrenal tissue development in *ff1b* morphants. The morphological defects of *ff1b* morphants could be mimicked by treatment with aminoglutethimide, an inhibitor of *de novo* steroid synthesis. Based on these data, we propose that *ff1b* is required for the development of the steroidogenic tissue of the interrenal organ.

Keywords: Interrenal; *ff1b*; Steroidogenesis; Aminoglutethimide; Osmoregulation; Morpholino; *3β-hsd*; Adrenal

Introduction

The adrenal glands and their homologs are the key endocrine tissue involved in mediating the stress response in vertebrates. The basic design of the adrenal glands has gained in structural organization during the course of vertebrate evolution, from the dispersed islets of chromaffin cells and presumptive adrenocortical tissues of the Agnathans (Hardisty, 1972; Jones and Mosley, 1980) to the encapsulated, closely juxtaposed, layered structure of the adrenocortical and medullary tissues of the mammalian adrenal glands (Hartman and Brownell, 1949; Holmes and Phillips, 1976; Idelman, 1978; Lofts, 1978; Balment et al., 1980). In teleosts, the adrenocortical cells are embedded in the cephalic regions of the kidney, commonly referred to as the "head kidney." The head kidneys of most teleosts are bilateral structures situated at the anterior end of the opistonephroi. In the order *Cypriniformes*, to which the zebrafish belongs, the adult head kidney consists of a mixture of steroidogenic or interrenal cells interspersed with hematopoietic and chromaffin cells (Nandi, 1962; Jones and Mosley, 1980). Anatomically, the head kidney commences caudal to the last gill slit and may extend posteriorly to the level of the second or third somite. Although a considerable amount of variation in topological arrangement occurs between different species (Nandi, 1962; Jones and Mosley, 1980), the adrenal homologs of teleosts are generally located around the posterior cardinal veins and their tributaries, and vascularized by branches of the dorsal aorta in both juveniles and adults (Giacomini, 1934; Nandi, 1962; Jones and Mosley, 1980; Hathaway and Epple, 1990; Hanke and Kloas, 1995; Reid et al., 1995). It has been proposed that the topographic position of the adrenocortical tissues within the kidney, their relations with blood vessels, and the relations between chromaffin and steroidogenic cells have important functional implications (Gallo et al., 1993; Hanke and Kloas, 1995; Reid et al., 1995), and these relationships have

* Corresponding author. Fax: +65-6779-2486.

E-mail address: dbscwk@nus.edu.sg (W.-K. Chan).

0012-1606/03/$ – see front matter © 2003 Elsevier Science (USA). All rights reserved.

doi:10.1016/S0012-1606(03)00219-7

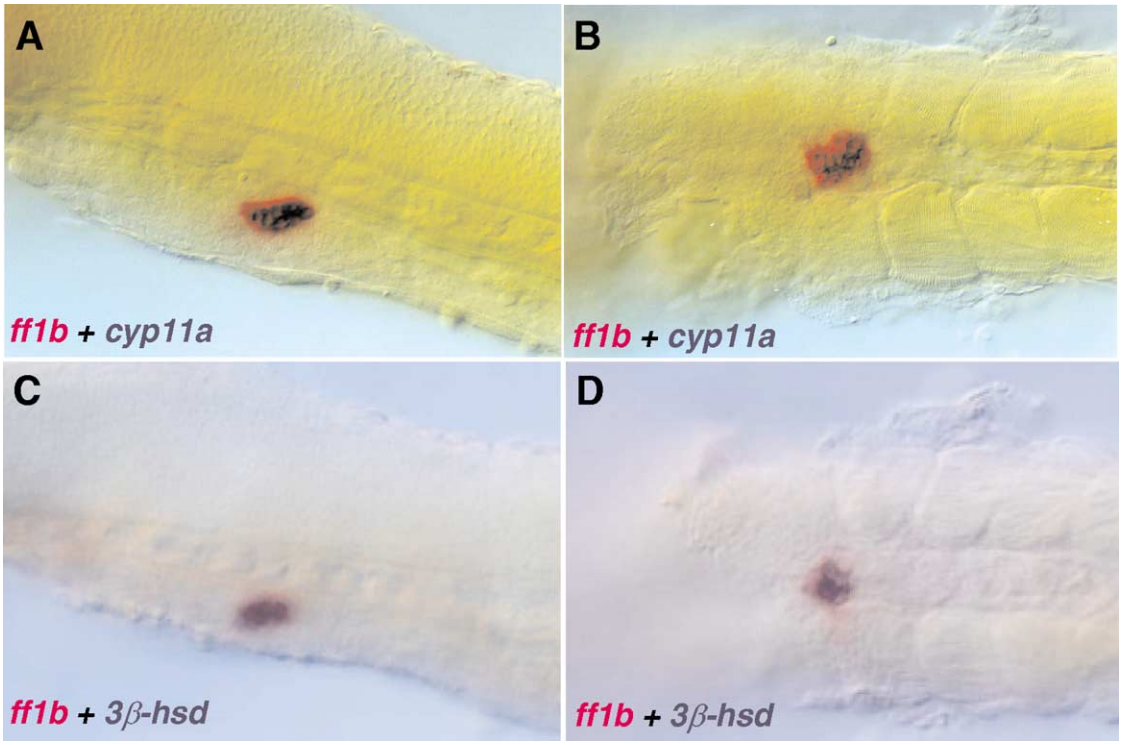

Fig. 1. Expression of *ff1b* in the interrenal organ. Whole-mount ISH with probes shown at bottom left of each panel. Lateral (A, C) and ventral (B, D) views of embryos. All embryos are at 36 hpf. (A, B) Double ISH for *ff1b* (red) and *cyp11a* (dark blue). (C, D) Colocalization of *ff1b* (red) and *3β-hsd* (dark blue).

been studied in a number of teleost species (Grassi Milano et al., 1997).

The adrenocortical steroidogenic cells and the medullary chromaffin cells differ in embryological origin and secrete different products (Hanke and Kloas, 1995). The chromaffin cells are derived from the neuroectoderm and migrate to the head kidney where they secrete mainly adrenaline and noradrenaline, although bioactive peptides and other amines may also be produced (Reid et al., 1995). The steroidogenic cells are derived from the mesodermal lineage that also gives rise to steroid-producing cells of the gonads. It has been proposed that the adrenocortical (interrenal) blastema in reptiles, birds, and mammals originate from the intermediate mesoderm, specifically from dedifferentiating, abortive, or vestigial pro/mesonephric units (Wrobel and Süβ, 1999). In these animals, vestigial nephrostomial tubules or their undifferentiated precursors form the first visible source of the adrenocortical blastema. Subsequent dedifferentiation of the Malpighian corpuscles and mesonephric tubules may also contribute to the development of the adrenocortical tissue. Guided by as yet unidentified molecular cues, these tissues migrate and coalesce at the cephalic end of the metanephric kidney to form the adrenal or interrenal glands. However, in anamniotes, the interrenal tissues are often not topologically separated from the opistonephroi. Instead, they may be embedded in the opistonephroi, as in cyclostomes, elasmobranch, and anurans, or are dispersed in the head kidneys as in teleosts (Balment et al., 1980).

Several genes have been identified to be pivotal for adrenal development (reviewed in Parker and Schimmer, 2001). In particular, the functions of three transcription factors, SF-1, Dax-1, and WT-1, have been studied and were found to be absolutely required for proper adrenal development. These genes are expressed in the earliest adrenogonadal primordium and act in the same developmental pathway to direct proper adrenal development. The importance of these genes in adrenal development can be seen in mouse knockout studies and human loss-of-function mutations in these genes. SF-1 knockout mice lack adrenal development and die perinatally from adrenocortical deficiency (Luo et al., 1995; Sadovsky et al., 1995). Mice lacking Dax1, however, do not exhibit adrenocortical deficiency and show apparently normal development of the adrenal cortex although the expression of *Cyp11A1* in the zona fasciculata is reduced compared with wild-type (Yu et al., 1997). In contrast, loss of DAX-1 function in human leads to much more severe effects on adrenal development. Patients with AHC, the condition associated with mutations in DAX-1, present with primary adrenocortical insufficiency. Their adrenal cortices show absence or near absence of adult zones (Zhang et al., 1998). In human, WT1 mutations lead to congenital abnormalities of urogenital development. Mouse knockout studies confirmed the importance of WT1, as animals homozygous for a null allele lacked kidneys, gonads, and adrenals (Kreidberg et al., 1993; Moore et al., 1999).

In contrast to mammalian adrenal development, virtually no information is available on the molecular determinants involved in interrenal development in teleosts. We have previously described the isolation of the zebrafish *ftz-fl* gene, *ff1b*, which shows strong homology to mammalian SF-1 and is expressed in discrete cell clusters in the midtrunk and diencephalon (Chai and Chan, 2000). We report herein the identification of *ff1b* as the earliest known molecular marker for teleost interrenal development. Using double ISH for *ff1b* and the steroidogenic markers *cyp11a* and *3β-hsd*, we showed that the expression of *ff1b* precedes the onset of steroidogenic identity during the ontogeny of the interrenal. Disruption of the *in vivo* gene activity of *ff1b* by antisense morpholino knockdown produced larval morphological phenotypes that are suggestive of impaired interrenal function. Histological analyses revealed that interrenal development in *ff1b* morphants has been disrupted. These lines of evidence implicate a direct involvement of *ff1b* in zebrafish interrenal development. The results from this study are also highly reminiscent of findings from mouse SF-1 knockout studies, in which SF-1 null mice demonstrated a complete lack of adrenal development (Luo et al., 1994; Sadovsky et al., 1995; Shinoda et al., 1995). The commonality between these two systems suggests a conserved regulatory program for adrenocortical development over more than 400 million years of evolution.

Materials and methods

Fish culture and embryo collection

Fish stocks were maintained in the fish facility of the Institute of Molecular Agrobiology, Singapore. Embryos were obtained by natural spawning and cultured in embryo medium at 28.5°C (Westerfield, 2000). Staging of embryos was carried out according to Kimmel et al. (1995). Embryos meant for histological analysis were cultured in 0.03% phenylthiourea (Sigma) solution from 18 h postfertilization (hpf) to inhibit melanin pigment formation.

Whole-mount In situ hybridization

Whole-mount *in situ* hybridization (ISH) was performed as previously described (Chai and Chan, 2000). Digoxigenin- or fluorescein-labeled riboprobes were synthesized from *Nco*I linearized *ff1b* plasmid by using *Sp6* RNA polymerase. Digoxigenin-labeled riboprobes were synthesized from plasmid containing zebrafish cDNAs for *proinsulin, cyp11a, 3β-hsd, dβh, prox1,* and *wt1*. Plasmids for *cyp11a, dβh,* and *prox1* were linearized with *Nco*I and transcribed with *Sp6* polymerase. *3β-hsd* and *proinsulin* plasmids were linearized with *Xho*I and *SphI*, respectively, and transcribed with *Sp6* polymerase. *Wt1* plasmid was linearized with *Spe*I and transcribed with *T7* polymerase. DIG-labeled riboprobes were detected with alkaline phosphatase-conjugated anti-DIG antibody (Roche) and visualized with NBT/BCIP (Promega), while fluorescein-labeled probes were detected by alkaline phosphatase-conjugated anti-fluorescein antibody (Roche) and visualized with Fast Red (Sigma). For two-color ISH, inactivation of the first antibody was performed by incubating the stained embryos in 100 mM glycine, pH 2.2, for 10 min followed by four washes with PBST for 10 min each before proceeding with the blocking step prior to incubation with the second antibody. The *3β-hsd* plasmid, pPCRIIHSD5, was kindly provided by Prof. B.C. Chung (Academia Sinica, Taipei, Taiwan; Lai et al., 1998). The *dβh* plasmid, pGTzfDβH, was a kind gift of Lam E.C.S and Assoc. Prof. V. Korzh (Institute of Molecular and Cell Biology, Singapore). The *cyp11a* plasmid contains a PCR fragment obtained using the primers, cyp11af (5′-GACAGTACTTCAAGAGCCTGG-3′), and cyp11ar (5′-CTATCTGCTGGCATTCAGTGG-3′), which are based on the sequence published by Lai et al. (1998).

Stained embryos were postfixed in 4% PFA and washed two times for 15 min in PBST. This is followed by tissue clarification in 50% glycerol in PBS. Specimens were mounted on glass slides with cover slips and photographed under Normaski optics on an Olympus AX710 microscope system.

Chromogenic histochemical staining for 3β-Hsd

Histochemical staining for 3β-Hsd was performed on whole embryos by using a protocol adapted from Levy's method as described by Grassi Milano et al. (1997). Embryos were fixed for 1 h at RT in 4% paraformaldehye in PBS and washed twice with PBST. Chromogenic reaction was incubated at RT in staining solution containing 0.1 mg/ml of the 3β-Hsd substrate, etiocholan-3β-ol-17-one (Sigma), 1.5 mg/ml β-nicotinamide adenine dinucleotide (NAD), 1 mg/ml bovine serum albumin (BSA), 1% N,N dimethyl formamide, 8.75 mM EDTA, and 1 mg/ml NBT in PBS. Reactions were monitored until sufficient signal intensities were obtained (3–8 h, depending on embryonic/larval stage). Staining reactions were terminated by washing in PBST followed by fixing in 4% PFA/PBS for 1 h. In control experiments, the substrate was omitted.

Treatment of embryos with aminoglutethimide

Crystalline aminoglutethimide (Sigma) was first dissoved in 0.2 N HCl to a concentration of 0.2 M and then diluted to 1 or 0.1 mM in egg water. The volume of 1 M Hepes (pH 7.9) required to adjust the 1 mM aminoglutethimide solution to pH 7.4 was determined, and equal amounts were added to other embryo cultures in the same

experiment to control for any effects that may be caused by Hepes. The final concentration of Hepes added was calculated as 2.5 nM and did not produce any observable defects in embryos. Embryos were treated from 8 hpf.

Microinjection of morpholino oligonucleotides

Morpholino oligonucleotides (morpholino) were synthesized at Genetools LLC. A stock solution of 4 mM was prepared by dissolving the lyophilized powder in ddH_2O. The required injection concentration was diluted from this stock in 1× Danieau solution containing 0.25% phenol red.

Freshly laid embryos were collected in egg water (Westerfield, 2000) and transferred onto a glass microscope slide with a plastic transfer pipette. Embryos were positioned into suitable orientations for microinjection following which excess water surrounding the embryos was removed by aspiration with a pipette. Morpholino solutions (4.6 nl) were delivered from the vegetal pole into the yolk directly underlying the blastodisc. Micropipettes were prepared from 10-cm borosilicate glass capillaries with an internal diameter of 0.58 mm (Sutter Instrument) on a Model P-97 Flaming/Brown Micropipette puller (Sutter Instrument). Microinjection was performed by using a Nanojet injector (Drummond). After microinjection, embryos were cultured in egg water containing a few drops of 0.02% methylene blue to prevent fungal growth.

Histology on embryos and larvae

Plastic sectioning

Embryos were embedded in 1.5% Bacto–Agar (Difco) prepared in PBS. Trimmed agar blocks were processed and embedded in Historesin according to the protocol provided with the Leica Historesin Embedding Kit. Sections of 6-μm thickness were cut with glass knives using a Leica RM 2055 Microtome (Leica). Sections were stained with Harris' Hematoxylin followed by Toluidine Blue according to protocol published by Energy Beam Sciences (http://www.ebsciences.com/papers/papers.htm#plastic). Micrographs were acquired either in print photography or electronically by using an Olympus AX710 microscope system equipped with an Olympus U-CMAD-2 CCD camera.

Cryostat sectioning

Samples were prepared for cryostat sectioning essentially as described in the Zebrafish Book (Chapter 8; Westerfield, 2000). Sections of 10-μm thickness were collected on a Leica CM1900 Cryostat (Leica). Print or electronic micrographs were acquired on an Olympus AX710 microscope system equipped with an Olympus U-CMAD-2 CCD camera.

Results

ff1b is expressed during ontogenic development of the interrenal organ

We have previously described the embryonic expression profile of *ff1b* and established that *ff1b*-expressing and pancreatic islet cells do not show any overlap and are clearly distinguishable from each other (Chai and Chan, 2000). Based on the high sequence homology between *ff1b* and mammalian *SF-1*, we asked if the *ff1b*-expressing cells could play a potential role in the development of steroidogenic tissue of the zebrafish interrenal organ. To investigate this possibility, the zebrafish homologs of known adrenocortical steroidogenic genes, *cyp11a* and *3β-hsd*, were isolated by RT-PCR for colocalization analysis with *ff1b*. *Cyp11a* encodes the P450SCC enzyme, which catalyzes the first, rate-limiting step in de novo steroid synthesis, i.e., the conversion of cholesterol to pregnenolone in the inner mitochondrial membrane and is known to be highly conserved throughout vertebrate evolution (Bourne, 1991; Selcer and Leavitt, 1991). *3β-hsd* encodes 3β-Hydroxysteroid dehydrogenase/Δ^5-Δ^4-isomerase, which catalyzes the oxidation and isomerization of 3β-Hydroxy-Δ^5-steroids, such as pregnenolone and dehydroepiandrosterone, into the Δ^4-ketosteroids progesterone and androstenedione, respectively. Double ISH showed considerable overlap in expression pattern between *ff1b* and both *cyp11a1* (Fig. 1A and B) and *3β-hsd* (Fig. 1C and D). The steroidogenic enzyme genes appeared to be expressed by an inner subpopulation of cells within the *ff1b*-expressing cluster. The onset of expression of *cyp11a1* and *3β-hsd* lagged behind that of *ff1b* by approximately 1.5 h, first appearing between 28.5 and 30 hpf (data not shown).

In addition to establishing the presence of steroidogenic gene transcripts in the interrenal cells, we performed experiments to visualize enzymatic activity of 3β-Hsd in these cells. In the presence of its substrates, such as dehydroepiandrostenedione, 3β-Hsd transfers protons to a proton acceptor such as tetrazolium salts to produce an insoluble diformazan precipitate. This histochemical reaction, using NBT as a color substrate, is commonly used for the specific detection of 3β-Hsd activity in adrenal/interrenal or testicular tissues (Grassi Milano et al., 1997; Contreras and Ronco, 1994). We used this method for whole-mount detection of 3β-Hsd activity in zebrafish embryos between 24 and 30 hpf at hourly intervals, at 36 hpf, as well as in larvae from 2 to 7 dpf at daily intervals. The earliest sign of 3β-Hsd activity was evident at around 29 hpf. Only embryos at 36 hpf and larvae from 2 to 7 dpf are shown (Fig. 2A–G). The sites of 3β-Hsd histochemical staining coincided exactly with the sites of occurrence of 3β-Hsd transcripts, thereby establishing them as interrenal cells. The number of 3β-Hsd-positive cells could be seen to increase from 36 hpf to 7 dpf. Beginning from 3 dpf, dispersal of the main cell cluster became evident, giving rise to a smaller

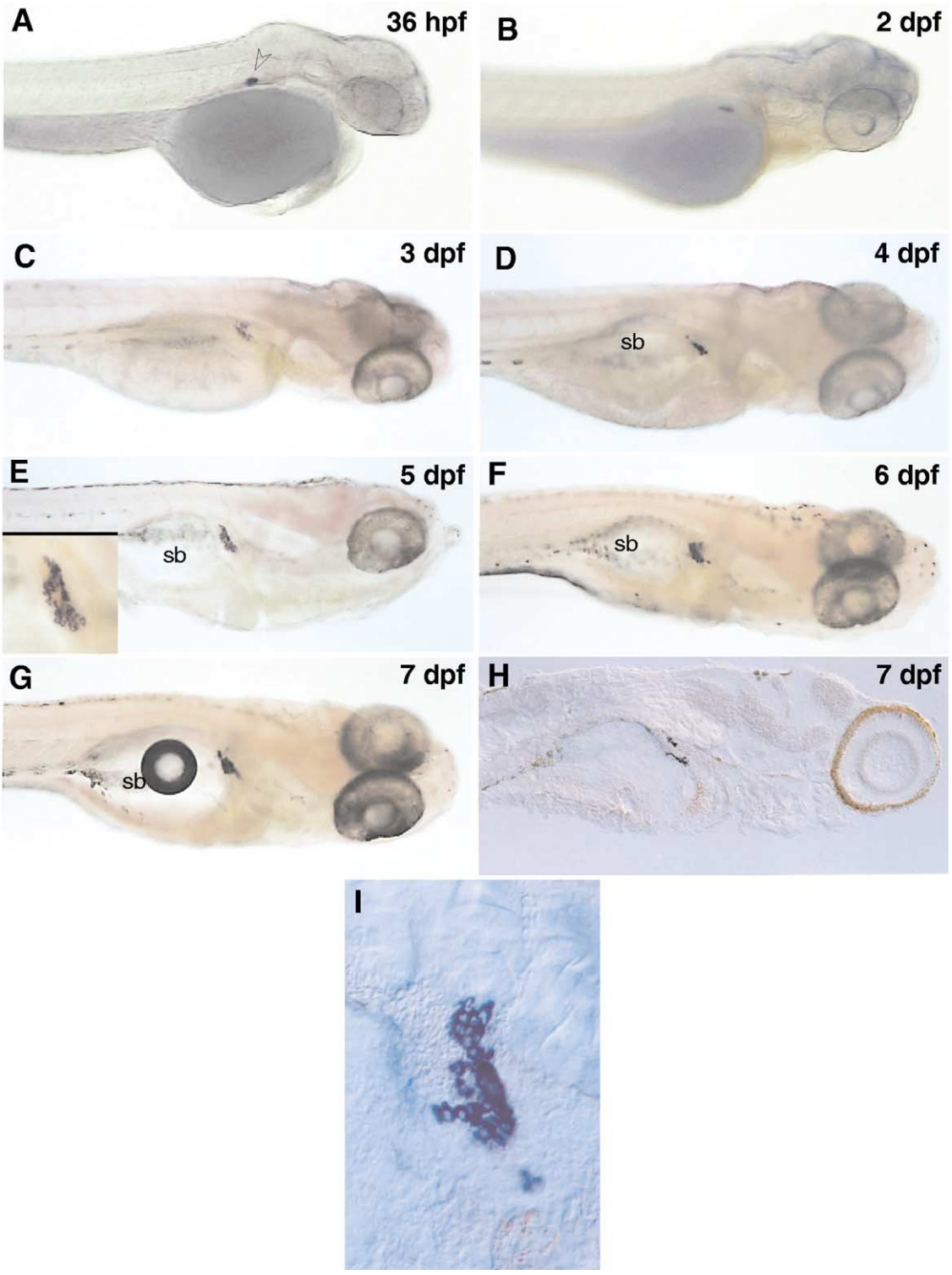

Fig. 2. Ontogeny of the interrenal organ shown by chromogenic detection of endogenous 3β-Hsd enzymatic activity. Dorsolateral (A–D, F, G) and lateral (E) views of embryos subjected to whole-mount chromogenic 3β-Hsd enzymatic reaction from 1-7 dpf. The interrenal organ is indicated by an open arrowhead in (A). Inset in (E) is a close-up view of the interrenal organ at 5 dpf. (H) Sagittal cryosection of a 7 dpf larva positively stained for 3β-Hsd. (I) Magnified view of sagittal cyosection of 7 dpf larva showing cellular morphology of the interrenal. sb, swim bladder. (Note: Embryos were photographed from the right in contravention of standard convention in order to provide a clearer view of the interrenal organ as it is displaced to the right of the midline.)

cluster located to the left of the midline (Fig. 2C). This was observed in an increasing number of larvae during subsequent days of growth. When inflation of the swim bladder became apparent at around 4 dpf, the interrenal cell clusters could be seen tightly compressed against the dorsal tip of the swim bladder (Fig. 2D). Cryosections of stained 7 dpf

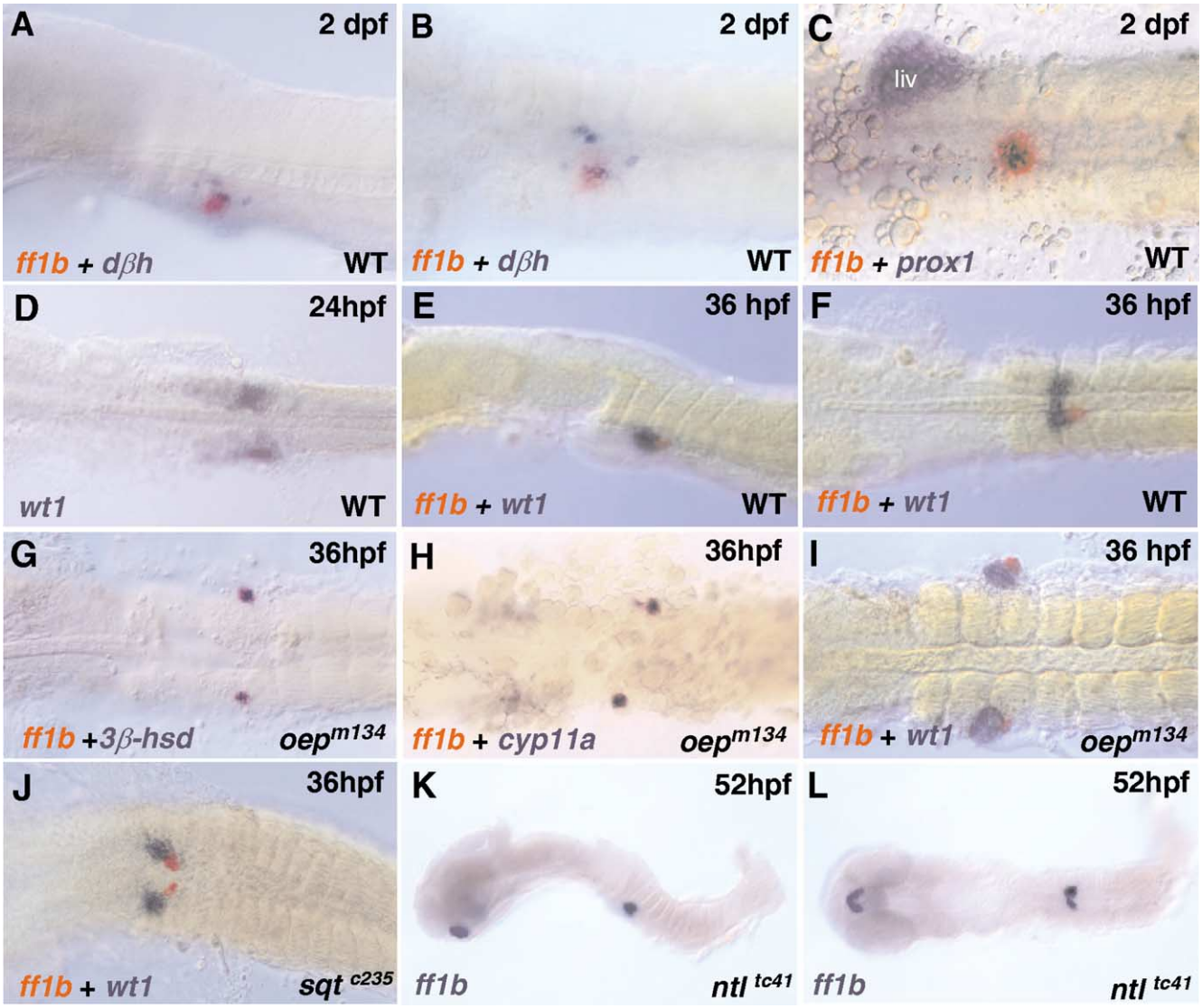

Fig. 3. Other cell types associated with interrenal tissue and expression of *ff1b* in midline signaling mutants. (A, B) Double ISH for *ff1b* (red) and the noradrenegic marker *DβH* (dark blue), which is expressed by chromaffin cells. (C) Ventral view of overlap of expression of *ff1b* (red) and *prox1* (dark blue) in the interrenal. Single ISH for the pronephric marker *wtl* at 24 hpf (D) and double ISH for *ff1b* (red) and *wt1* (dark blue) at 36 hpf (E, F). Ventral views of 36-hpf oep^{m134} embryo following double ISH colocalization of *ff1b* (red) with 3β-hsd (G, dark blue) and *cyp11a* (H, dark blue). Double ISH for *ff1b* (red) and *wt1* (dark blue) in oep^{m134} (I) and sqt^{c235} (J) embryos. (K, L) ISH for *ff1b* in 52 hpf ntl^{tc41} embryos.

larvae-showed the interrenal cells as having a squamous morphology and large nuclei characteristic of steroidogenic cells (Fig. 2I).

The interrenal tissue is intermingled with chromaffin cells and shows evidence of vascularization during development

In teleosts, the interrenal and adrenomedullary cells are known to intermingle to varying extent in the head kidney, depending on the species (Grassi Milano et al., 1997). Accruing evidence from studies performed in mammals and amphibians indicates that these two cell types are functionally dependent on one another (DeLean et al., 1984; Pratt et al., 1985; Ehrhart-Bornstein et al., 1995; Haidan et al., 1998; Bornstein et al., 1990, 2000; Shepherd and Holzwarth, 2001). Paracrine control of catecholamine release from chromaffin stores by cortisol has been shown in the rainbow trout (Reid et al., 1996). Perfusion studies on carp head kidney with acetylcholine and its agonists or antagonists suggest that there may be crosstalk between the chromaffin and interrenal cells (Gfell et al., 1997). The anatomical relationship between the two types of cells in the head kidney of the embryonic zebrafish was studied. Dopamine β-hydroxylase (DβH) converts dopamine to noradrenaline and is expressed in the chromaffin cells of teleosts (Reid et al., 1995; Grassi Milano et al., 1997). Double ISH of *ff1b* and *dβh* showed several clusters of noradrenergic neurons

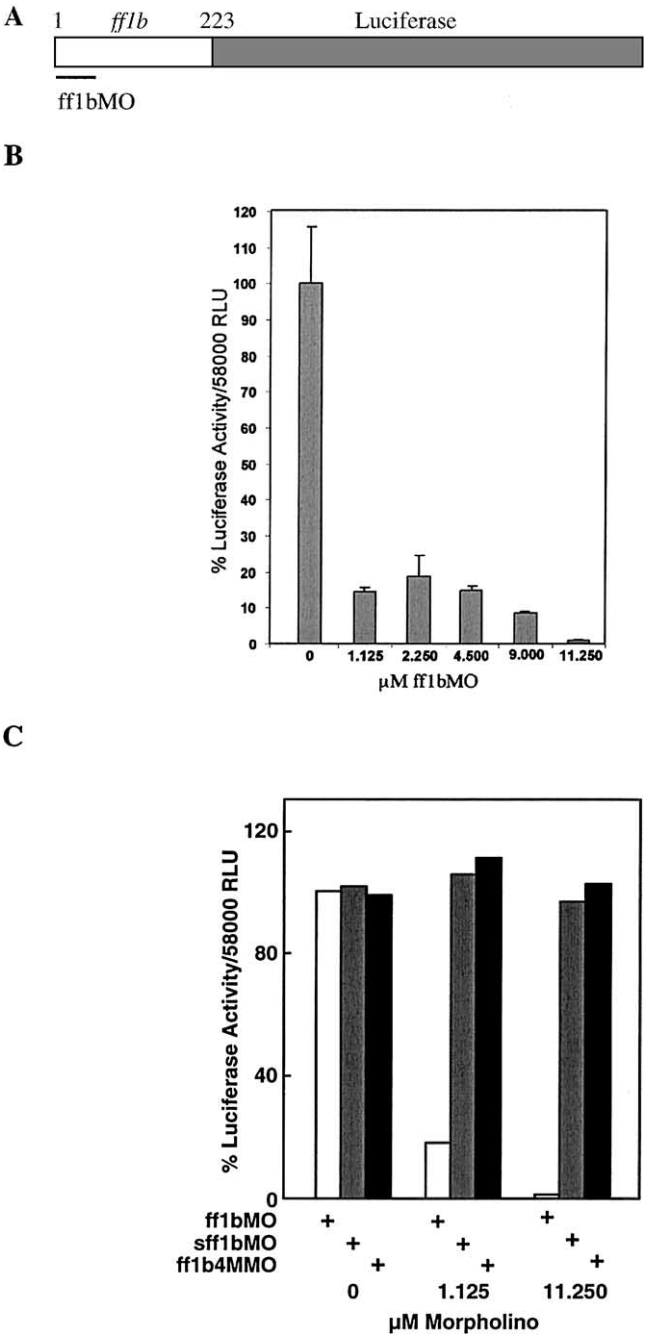

Fig. 4. Specificity of ff1bMO in blocking translation of *ff1b-Luc* mRNA. (A) Diagram of the *ff1b-Luc* fusion construct. (B) *In vitro* assay for ff1bMO efficacy in blocking Luc expression from a *ff1b-Luc* fusion construct. A *ff1b-Luc* fusion plasmid was constructed by inserting a 718-bp *ff1b* fragment containing the ff1bMO target site upstream of the luciferase gene. The construct was coinjected with ff1bMO into one- to two-cell-stage embryos to give final concentrations ranging from 0 to 11.25 μM. Twenty embryos were harvested for luciferase assay for each dosage injected. The experiment was repeated three times, and the mean ($\pm$SD) is shown. (C) Injection of ff1bMO, but not sff1bMO or ff1b4MO, into one- to two-cell-stage embryos reduced luciferase expression from the *ff1b-Luc* fusion construct.

occurring in the anterior kidney region and that they have a dispersed distribution (Fig. 3A and B). One cluster was associated tightly with *ff1b*-positive cells (Fig. 3B).

Double ISH was also carried out for *ff1b* and *prox1*. Prox1 is a homeobox protein that is required for endothelial budding of veins that contribute to the development of the lymphatic system in mouse (Wigle and Oliver, 1999) and is widely expressed in compartments of all three germ layers where it is believed to play an important role in endothelial differentiation (Rodriguez-Niedenfuhr et al., 2001). In zebrafish, *prox1* expression pattern is highly dynamic, occurring in various tissue compartments, such as the lens, ventral hindbrain, trigeminal ganglia, otic vesicle, heart, and liver (Glasgow and Tomarev, 1998). Double ISH for *ff1b* and *prox1* revealed a localized expression domain of *prox1* within the core of *ff1b*-positive cells in the interrenal gland at 36 hpf (Fig. 3C), which persists up to 48 hpf.

The zebrafish interrenal tissue and pronephros may be developmentally coupled

The development of the adrenal gland and the kidney are tightly linked in higher vertebrates, both deriving from the same mesodermal precursors. Since the location of *ff1b*-expressing cell cluster corresponds closely to the described location for the zebrafish pronephros (Drummond et al., 1998), we performed double ISH for *ff1b* and the pronephric marker *wt1* to reveal their relative anatomical positions. *Wt1* is an essential regulator of nephrogenesis in higher vertebrates (Kreidberg et al., 1993; Torres et al., 1995) as well as in amphibians (Carroll and Vize, 1996; Semba et al., 1996; Heller and Brandli, 1997). In addition, it has been implicated in the development of the mammalian adrenal glands (Moore et al., 1999; reviewed in Parker and Schimmer, 2001) and has been shown to be an interaction partner for SF-1 (Nachtigal et al., 1998). Zebrafish *wt1* is first expressed in the intermediate mesoderm at the level of somites 1–3 (Drummond et al., 1998). At 24 hpf, *wt1* expression became restricted to the forming nephron primordia, which were visible as bilateral cords of cells parallel to the midline at the level of somites 1–3 (Fig. 3D). At 30 hpf, the expression domains of *wt1* condensed into two clusters located very close to the midline (not shown). By 36 hpf, these two clusters coalesced at the midline beneath the notochord at the level of the second myoseptum (Fig. 3E and F). This region represents the position of the future glomerulus (Drummond et al., 1998). At 36 hpf, the *ff1b*-positive cell cluster could be seen in contact with the right half of the *wt1* cluster at a slightly caudal position (Fig. 3E and F). The

Table 1
Number (and percentage) of ff1bMO- and sff1bMO-injected zebrafish larvae retaining interrenal 3β-Hsd enzymatic activity

	n	ff1bMO	*n*	sff1bMO
3 dpf	268	23 (8.6%)	287	286 (99.6%)
5 dpf	315	8 (2.5%)	313	312 (99.6%)
7 dpf	241	11 (4.6%)	239	236 (98.7%)

n, number of larvae examined.

Table 2
Classification of *ff1b* morphant phenotype at 7 dpf

Phenotype	Class A*	Class B	Class C	Class D
Mouth	protruding	protruding	shortened snout	shortened snout
Swim bladder inflation	full	none	none	none
Heart beat	strong	slow	slow	slow
Pericardial sac	normal	edema	edema	edema
Blood flow	rapid	slow	none	none
Yolk sac	normal	normal	edema	severe edema
Otic sac	normal	normal	slight edema	severe edema
Yolk absorption	complete	delayed	delayed	delayed
Blood islands	none	none	ventral tail	ventral tail

* Class A phenotype resembles wildtype.

anatomical relationship between *ff1b*- and *wt1*-expressing structures in zebrafish is highly reminiscent of the association between the adrenal glands and kidneys in mammals, although these organs are apparently unpaired in the zebrafish.

Interrenal development in zebrafish mutants with midline signaling defects

Several large-scale zebrafish mutagenesis screens have yielded mutants defective in the formation, patterning, or signaling of midline structures and they are collectively known as the midline signaling mutants (Brand et al., 1996; Karlstrom et al., 1996). The midline structures, consisting of the floor plate and the notochord, play important roles in patterning surrounding structures such as the somites and the overlying neural tube (reviewed by Dodd et al., 1998; Kodjabachian et al., 1999). Several mutations in this group have been mapped to genes encoding signaling molecules that mediate the inductive interactions between different germ layers during patterning of the midline.

In zebrafish *one-eyed pinhead (oep)* mutant, the prechordal plate fails to develop, leading to cyclopia and defects in the ventral forebrain. *oep* mutants also show defects in floor plate and endoderm formation (Schier et al., 1997; Strahle et al., 1997). An almost identical phenotype is observed in the *cyclops (cyc)* and *squint (sqt)* double mutant (Feldman et al., 1998; Sampath et al., 1998). Both *cyc* and *sqt* encode TGFβ-like molecules closely related to mouse *Nodal* (Conlon et al., 1994; Zhou et al., 1993; Feldman et al., 1998; Sampath et al., 1998; Rebagliati et al., 1998). Mutants for either gene lack the floor plate (Hatta et al., 1991; Feldman et al., 1998), while double mutants lack all axial mesoderm, suggesting that the two genes play partially redundant roles. The proper formation of the notochord in zebrafish depends on another gene, *no tail (ntl)*. The *ntl* locus is the homolog of the mouse *Brachyury* gene (Schulte-Merker et al., 1992; Halpern et al., 1993; Schulte-Merker et al., 1994).

To study whether *ff1b* expression is affected by mutations in midline signaling genes, the expression pattern of *ff1b* was examined in oep^{m134}, sqt^{c235}, and ntl^{tc41} mutants. Such analyses would also be able to reveal any genetic interaction between *ff1b* and the midline signaling genes as well as to provide information about the developmental origin of *ff1b*-expressing cells. In 36-hpf oep^{m134} embryos, *ff1b* expression in the trunk was observed as two lateral clusters ventral to the third somite instead of a single cluster seen in wild-type embryos (Chai and Chan, 2000). The distance between the two clusters differed between embryos, most likely reflecting the varying penetrance of the mutation. Double ISH for *ff1b* and *3β-hsd* showed that expression of *3β-hsd* within each cluster was not affected despite the ectopic location of expressing cells (Fig. 3G). Similarly, the expression of *cyp11a* is not affected (Fig. 3H). Double ISH with *wt1* showed that convergence of the nephric primordial cells is impaired. Nevertheless, they remained closely associated with the *ff1b*-expressing clusters (Fig. 3I). In sqt^{c235} mutant embryos, *ff1b* expression occurred in bilateral clusters of cells close to the midline (Fig. 3J), similar to that observed for oep^{m134} embryos. Double ISH with *wt1* revealed that pronephric primordial cells fail to converge at the midline, as observed in oep^{m134} embryos. The relative position of *ff1b*- and *wt1*-expressing clusters is inverted in sqt^{c235} embryos when compared with oep^{m134} mutants. The convergence of *ff1b*-expressing clusters was less severely affected in sqt^{c235} embryos compared with oep^{m134} embryos. The convergence of *ff1b*-expressing clusters was affected to varying degree in ntl^{tc41} embryos, but as a whole, the effects are milder compared with oep^{m134} embryos.

Morpholino-mediated knockdown of endogenous ff1b gene function disrupts interrenal development

Microinjection of antisense morpholinos into single-cell zebrafish embryos has proven to be an effective method to achieve specific disruption of the function of a target gene. Morpholino-mediated effects remain potent in all cells throughout the first 50 h of development (Ekker, 2000; Nasevicius and Ekker, 2000). Morpholino-mediated gene knockdown was used to perturb the functions of *ff1b* during

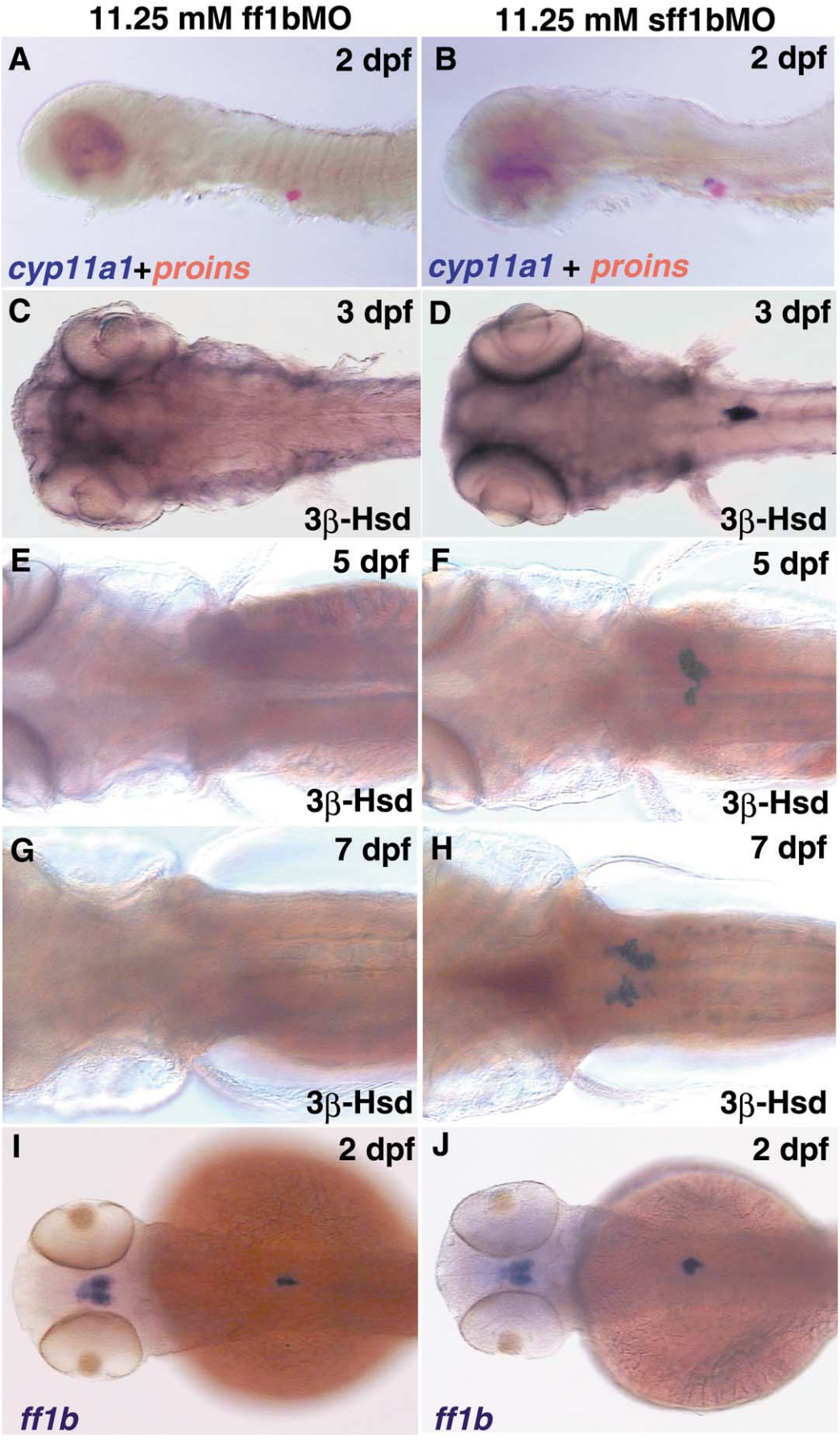
11.25 mM ff1bMO
11.25 mM sff1bMO
A
2 dpf
cyp11a1+proins
B
2 dpf
cyp11a1 + proins
C
3 dpf
3β-Hsd
D
3 dpf
3β-Hsd
E
5 dpf
3β-Hsd
F
5 dpf
3β-Hsd
G
7 dpf
3β-Hsd
H
7 dpf
3β-Hsd
I
2 dpf
ff1b
J
2 dpf
ff1b

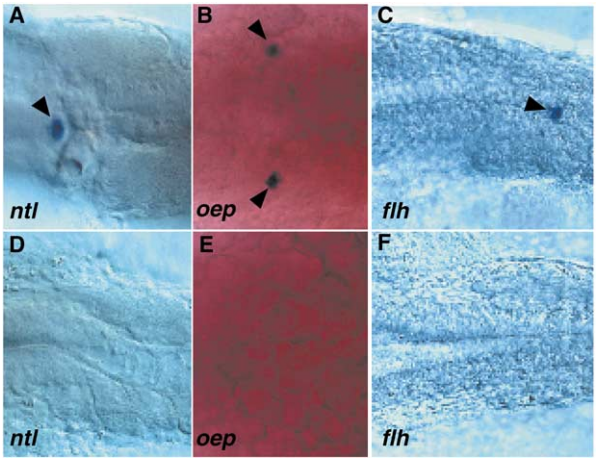

Fig. 6. Effects of *ff1b* morpholino injection on the expression of 3β-Hsd in midline signaling mutants. Dorsal view of *ntl*^{tc41}, *oep*^{m134} and *flh*^{tk241} mutant embryos microinjected with (A–C) 11.25 μM of sff1bMO, or (D–F) 11.25 μM of ff1bMO, at 32 hpf. Arrowheads in (A–C) indicate the position of the histochemical 3β-Hsd staining.

embryogenesis. An antisense morpholino, ff1bMO (5′-AATCCTCATCTGCTCTGAAGTC-3′), was designed complimentary to the start codon and 22 adjacent downstream bases of the *ff1b* mRNA. A sense-strand morpholino, sff1bMO (5′-GACTTCAGAGCAGATGAGGATT-3′), and a mutated antisense morpholino, ff1b4MMO (5′-AATCTCATCGCTCGAAGT CAT-3′) were designed as negative controls.

The efficacy of ff1bMO in targeting and blocking protein translation from *ff1b* transcripts was analyzed by a quantitative assay based on firefly luciferase reporter gene. A 718-bp *ff1b* cDNA fragment containing the ff1bMO target site, as well as the coding region for the first 233 amino acid residues of Ff1b, was fused in-frame to the 5′ end of a luciferase gene in a CMV promoter-driven expression vector to yield the plasmid pCMVff1bLuc (Fig. 4A). This plasmid construct was then coinjected with increasing amounts of ff1bMO or sff1bMO into live embryos. After allowing 24 h for embryonic growth and expression of the plasmids, embryos were harvested for Luc activity determination. Fig. 4B indicates that ff1bMO coinjection reduced luciferase expression from the *ff1b-Luc* fusion construct. Coinjection of 2.25 μM of ff1bMO per embryo reduced measured luciferase activity by 80%, while at the highest ff1bMO concentration (11.25 μM) injected, an almost 99% reduction was noted. Moreover, sff1bMO and ff1b4MMO at similar concentrations had no significant effects on the luciferase activity of pCMVff1bLuc-injected embryos (Fig. 4C). This indicates that the ff1bMO morpholino was effective in blocking translation from its target transcripts under physiological conditions.

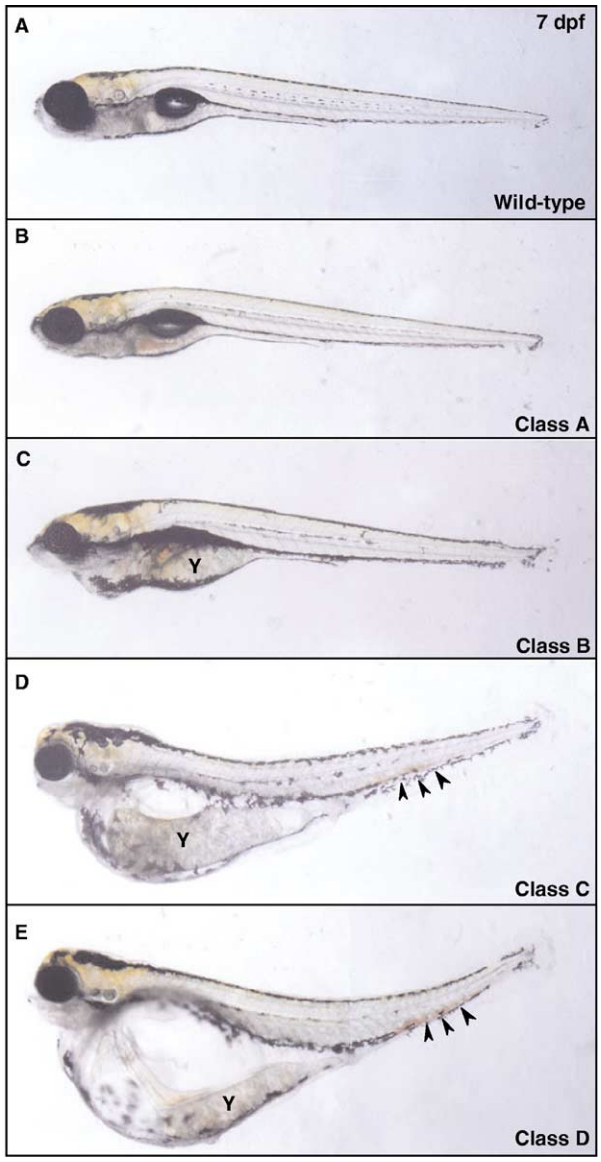

Fig. 7. Phenotypes of 7 dpf larvae resulting from microinjection of 11.25 μM ff1bMO per embryo. (A) Wild-type, (B) Class A, (C) Class B, (D) Class C, and (E) Class D phenotype. Arrowheads in (D) and (E) indicate blood island formation.

Morpholino knockdown of ff1b gene function downregulated expression of the steroidogenic genes, cyp11a and 3β-Hsd

In order to investigate the potential role of Ff1b in interrenal development, we first evaluated the effects of ff1bMO injection on the expression of the steroidogenic enzymes, *cyp11a* and *3β-hsd*, by ISH and chromogenic enzymatic reaction, respectively. Both genes have been shown to be expressed in the developing interrenal of the

Fig. 5. Effects of *ff1b* morpholino injection on the expression of *cyp11a*, 3β-Hsd, and *ff1b*. (A, B) Double ISH for *cyp11a* and *proinsulin* on embryos injected with 11.25 μM per embryo of (A) ff1bMO and (B) sff1bMO. Histochemical staining for 3β-Hsd activity in ff1bMO (C, E, G) and sff1bMO (D, F, H) injected larvae at 3 (C, D), 5 (E, F), and 7 dpf (G, H). ISH for *ff1b* in ff1bMO (I)-and sff1bMO (J)-injected 2-dpf embryos.

zebrafish. The effects of *ff1b* morpholino on the expression of the two genes were assessed by different methods, *cyp11a* at the transcriptional level by ISH for its transcripts, while 3β-Hsd was assayed at the translational level by histochemical detection of the enzymatic activity of its encoded protein.

Embryos microinjected with 11.25 μM of ff1bMO and sff1bMO were collected at 2 dpf for double ISH with *cyp11a* and *proinsulin* riboprobes. The inclusion of *proinsulin* detection serves to control for proper ISH technique. In our initial experiment, out of 50 embryos injected with 11.25 μM of morpholino, 5 ff1bMO- and 4 sff1bMO-injected embryos failed to show staining for both *cyp11a* and *proinsulin*. Injection of ff1bMO abolished *cyp11a* expression in 86.7% (39/45) of embryos, while at the same dosage, only 6.5% (3/46) of sff1bMO-injected embryos failed to show staining for *cyp11a* (Fig. 5A and 5B).

The effects of ff1bMO injection on *3β-hsd* expression were assessed by chromogenic detection of 3β-Hsd enzymatic activity. The use of an enzymatic assay provides an additional level at which morpholino effects are assessed viz at the level of protein function of a downstream effector. Embryos injected with 11.25 μM of ff1bMO and sff1bMO were collected at 3, 5, and 7 dpf for 3β-Hsd histochemical staining. Representative embryos from these experiments are shown in Fig. 5C–H. The results from two independent experiments are summarized in Table 1. Injection of ff1bMO significantly reduced the number of embryos showing 3β-Hsd activity in the interrenal. The mean percentages of 3β-Hsd-negative embryos were 91.4, 97.5, and 95.4% at 3, 5, and 7 dpf, respectively. Almost 100% of embryos injected with sff1bMO showed positive 3β-Hsd staining, thereby establishing the specificity of ff1bMO effects.

At all three time points analyzed, a portion of ff1bMO-injected larvae (from 2.5 to 8.6%) showed positive staining for 3β-Hsd (Table 1), indicating that the interrenal of these larvae had eluded the effects of morpholino. At 7 dpf, these ff1bMO-injected but 3β-Hsd-positive larvae displayed only Class A phenotype, which resembles the phenotype of wild-type. It is likely that the interrenal of these larvae had received suboptimal amounts of ff1bMO due to two possible reasons. Some morpholino may have been lost following microinjection due to back pressure of the embryo. This is in spite of the inclusion of phenol red in the injection mix to provide a visual indicator of the successful delivery of injected material. Dilution of the retained morpholinos may have resulted in concentrations too low to interfere with interrenal development and functions. Another explanation, though less plausible, may be that injected morpholino had not spread evenly throughout the embryos, thereby limiting its effects on the interrenal organ.

We have also investigated the effects of ff1bMO and sff1bMO in three midline mutants, oep^{m134}, ntl^{tc41}, and flh^{tk241}. The *floating head (flh)* mutant embryo lacks a notochord (Odenthal et al., 1996). Embryos injected with 11.25 μM of ff1bMO and sff1bMO were collected at 32 hpf for determination of 3β-Hsd activity. In oep^{m134}, ntl^{tc41}, and flh^{tk241} embryos, the injection of sff1bMO had no effects on the initiation of the interrenal primordium, as revealed by 3β-Hsd staining (Fig. 6A–C), while ff1bMO completely abolished the 3β-Hsd staining (Fig. 6D–6F). Furthermore, in the flh^{tk241} embryos, the appearance and merger of the bilateral interrenal primordia appeared not to be perturbed (Fig. 6C), which is similar to what we have described for ntl^{tc41} embryos.

Morpholino knockdown of ff1b gene function leads to impaired osmoregulation

Embryos microinjected with 11.25 μM of ff1bMO and sff1bMO were allowed to develop to larval stages and monitored for morphological changes. The phenotypes of the larvae could be grouped into four different classes based on the severity of observed defects (Table 2). Phenotypic changes begin to appear around 5 dpf, and were fully manifested by 7 dpf (Fig. 7C–E). Larvae were scored for phenotypes at 7 dpf, and then again at 10 dpf. The phenotypes at 10 dpf were essentially the same as those described for larvae at 7 dpf, with the exception that fluid accumulation had become more pronounced in some embryos and the yolk had been completely absorbed (Fig. 8A and B). The proportion of larvae displaying the different classes of phenotypes at 7 and 10 dpf is presented in Table 3.

By 5 dpf, some ff1bMO-injected larvae had begun to show signs of fluid accumulation in their body cavities, predominantly in the abdomen. At 7 dpf, varying degree of severity of subcutaneous edema could be seen. Slight increase in size was observed in mild cases (Class B), but in severe cases (Class C and D), fluid accumulation may occur to such an extent that body size increased to more than three times that of normal, restricting motility of the larvae. Curvature of the body axis was also evident in more severe cases, resulting in concavity of dorsal axis. Craniofacial deformities were often associated with the Class C and D phenotypes (Fig. 7D and E). Typical abnormalities included a shortened snout and protruding lower jaw. Edema of the optic sacs caused protrusion of the optic cup. As a result, optic nerves that were still connected to the optic cups become tautly stretched, which could be clearly observed at 10 dpf (Fig. 8A, inset). Edema of the pericardial sac likely interfered with cardiac pumping leading to slowing or cessation of heartbeat. Blood circulation ceased in individuals that lacked cardiac activity, and as a result, blood islands formed predominantly in the ventral tail (Fig. 7D and E). Inflation of the swim bladder was observed for individuals in Class A and B (Fig. 7B and C), but not for those in Class C and D (Fig. 7D and E). About 10% of control embryos injected with sff1bMO also displayed phenotypes associated with Classes B to D. No abnormal phenotype was observed for uninjected embryos.

Aminoglutethimide, an inhibitor of adrenal steroidogenesis, mimics ff1b morphant phenotypes

Excessive fluid accumulation in *ff1b* morphants suggests a dysregulation of osmoregulatory functions. Since the interrenal organ, through its secretion of corticosteroids, is known to be essential for osmoregulation in teleosts, we hypothesized that osmoregulatory phenotypes observed in *ff1b* morphants could have resulted from the loss of interrenal steroidogenic functions. Aminoglutethimide (AG) is a potent inhibitor of the P450SCC enzyme (Uzgiris et al., 1977; Whipple et al., 1978) and is used in the treatment of adrenal pathologies, such as Cushing's syndrome. AG is also known to inhibit aromatase activity (Thompson Jr. and Siiteri, 1974; Graves and Salhanick, 1979). Since P450SCC is the rate-limiting enzyme in steroid hormone synthesis, treating embryos with AG would be expected to inhibit de novo steroid synthesis in the interrenal organ, thereby effecting pharmacological interrenalectomy.

Treatment of embryos with 1 mM of AG, starting from 8 hpf, resulted in late larval phenotypes (Fig. 8E and F) that were remarkably similar to those shown by Class C and D *ff1b* morphants. Subcutaneous edema became evident in ~74% of the larvae from around 8 dpf. At 11 dpf, phenotypes including curvature of the body axis, edema of the cranial, optic, pericardial and yolk sacs, a shortened snout, and protrusion of the lower maxilla were clearly manifested (Fig. 8E and F). However, no blood island formation was noted in AG-treated larvae. Yolk sac edema in the most severely affected AG-treated larvae was less extensive compared with Class D *ff1b* morphants. The penetrance of AG treatment in inducing phenotype was, however, much higher than that caused by ff1bMO injection. This probably reflects the high diffusibility of AG. Treatment with 0.1 mM AG did not produce any phenotype that could be distinguished from wild type or buffer controls.

Morpholino knockdown of ff1b function disrupted interrenal development

Although the above data provide strong evidence for a direct role of *ff1b* in the transcriptional regulation of *cyp11a* and *3β-hsd* gene expression, it remains possible that the observed downregulation of these steroidogenic genes is due to a secondary effect arising from the loss of cells whose survival depended on *ff1b* functions. Alternatively, or perhaps in tandem, the loss of steroidogenic potential may have led to reduced tissue viability, thereby establishing a destructive loop. To investigate whether ff1bMO injection had affected tissues at the histological level, wild-type and ff1bMO-injected embryos and larvae were collected for detailed histological examination. Specimens at 30 hpf, 2, 3, 5, and 7 dpf were first subjected to 3β-Hsd histochemical staining, before being sampled for plastic sectioning. As morphant phenotypes have not yet become apparent prior to 7 dpf, embryos and larvae were randomly sampled for analysis. Larvae from morphant Classes A and D were sampled for examination at 7 dpf. For each stage, at least three specimens were sectioned, either two in cross-section and one in sagittal section or vice versa.

Photomicrographs of histological sections are shown in Fig. 9. The NBT precipitate produced by 3β-Hsd reaction remained insoluble in the interrenal of embryos of up to 3 dpf and persisted throughout plastic embedding. However, in older larvae, the precipitate readily dissolved during plastic infiltration and was no longer visible following hardening of the blocks. This may indicate a shift in the cytosolic properties of the interrenal cells, possibly an increase in hydrophobicity due to lipid accumulation.

At 30 hpf, the zebrafish interrenal, which was stained by NBT as a result of 3β-Hsd activity, appeared as a compact, oval-shaped cluster of cells situated just above the yolk and ventral to the third somite (Fig. 9A). In transverse section, it was displaced slightly to the right of the body axis (Fig. 9B). On the opposite side of the midline, a pouch in the yolk sac accommodated the gut epithelium. At 2 dpf, the interrenal gland appeared to be surrounded by a fibrillar capsule and had elongated along the AP axis (Fig. 9E and F). The gut and liver primordia were visible at this stage. No histochemical staining for 3β-Hsd was observed for ff1bMO-injected embryos at either 30 hpf (Fig. 9C and D), or 2 dpf (Fig. 9G and H).

At 3 dpf, the interrenal gland was clearly defined, forming a discrete structure (Fig. 9I). In transverse section, cells had acquired a birefringent appearance and showed very weak staining with both toluidene blue and hematoxylin (Fig. 9J), an indication of hydrophobicity most likely as a result of the accumulation of steroidal products. Also, the epithelial sheets of the swim bladder had become evident, caudal to the interrenal gland. The lumina of the gut and pneumatic duct began to expand at this stage (Fig. 9J). In ff1bMO-injected embryo, no structure resembling the interrenal was noticeable, although development of all other structures, such as the swim bladder, gut, and pneumatic duct, appeared to be normal (Fig. 9K and L).

The cellular organization of the interrenal tissue was evident at 4 dpf. It consisted of large, cuboidal cells with clearly stained nuclei. Although their cytoplasm was weakly stained, the interrenal cells could be readily visualized under Nomarski optics. In transverse view, the cells form two neat rows that were oriented at an oblique angle to the DV axis. Serial transverse sections reveal a similar cellular arrangement throughout the length of the organ (data not shown), suggesting that the interrenal is formed by a two-tiered cell layer at this stage. The interrenal gland contacts the cephalic end of the pronephric duct, which lies slightly caudoventral to it (Fig. 9M and N). The swim bladder was fully developed at this stage. In normal larvae, acquisition of swim bladder functions occurs between 3 and 4 dpf (Liu and Chan, 2002).

At 5 dpf, the interrenal gland had become a prominent structure. Blood vessels began to vascularize the organ, and

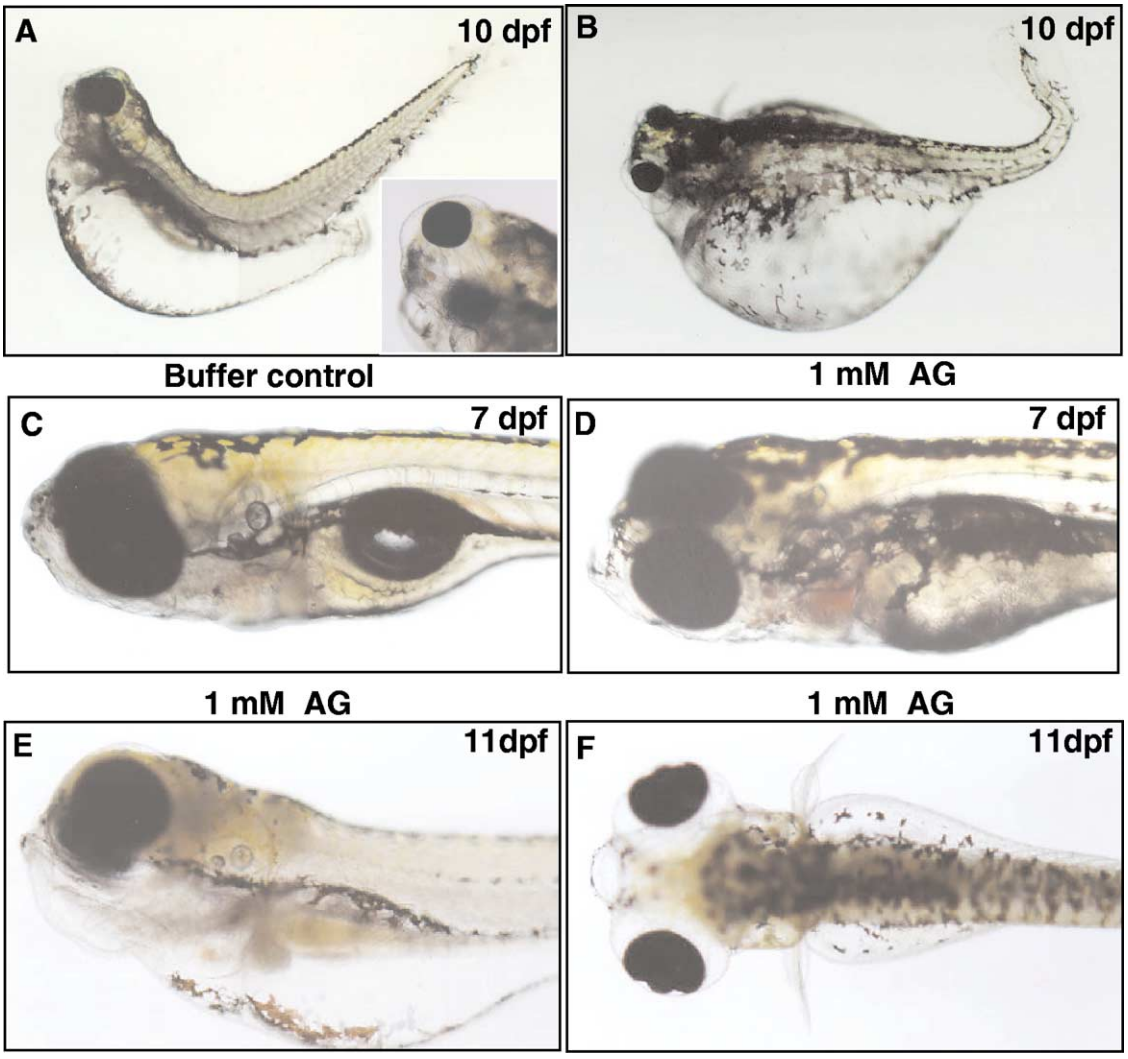

Fig. 8. Late larval *ff1b* morphant phenotypes are phenocopied by treatment with aminogluthemide (AG). (A) Class C and (B) Class D phenotypes at 10 dpf following microinjection of 11.25 μM of ff1bMO per embryo. Inset in (A) shows severe optic sac edema in a Class C larvae. (C–F) Phenotypic effects of AG treatment. (C) Buffer control at 7 dpf. (D) 7 dpf larva treated with 10^{-3} M of AG. (E, F) 11 dpf larva treated with 10^{-3} M of AG. Embryos were treated from 8 hpf.

sinuses could be observed between the two layers of cells. These vessels probably arose from the posterior cardinal vein. Blood cells were easily distinguishable by their dark-staining, elliptical nuclei and their thin cytoplasm that is stained turquoise by Toluidine blue as could be seen in the atrium of the heart (Fig. 9M). By examining serial sections, only a single pronephric tubule can be found. It appeared as a granular structure, extending caudally along the dorsal or right side of the gastrointestinal tract. Its anterior end contacted the interrenal gland. The interrenal was clearly absent in ff1bMO injected-larvae (Fig. 9Q and P). Its normal anatomical location was occupied by blood sinuses or empty cavities in *ff1b* morphants. No apparent difference was noted in other organs, such as pronephros, swim bladder, or liver. A distinct glomerulus could be observed (Fig. 9O).

In wild-type larvae, the interrenal cells had undergone considerable proliferation between 5 and 7 dpf. The bilayer cell arrangement seen in the 4 and 5 dpf had given rise to branching cords of cells that spread ventrally (Fig. 9R). As observed for whole-mount 3β-Hsd staining (Fig. 2G), a smaller group of cells had appeared on the left of the

Table 3
Percentages of morphants exhibiting different classes of phenotypes at 7 and 10 dpf

Age (dpf)	Morpholino	Percentage of embryos (%)				*n*	Dead
		Class A	Class B	Class C	Class D		
7	ff1bMO	47.0	20.9	17.8	14.3	321	0
	sff1bMO	89.3	5.3	3.2	2.1	281	0
	ff1b4MMO	97.6	1.5	0.9	0	344	1
10	ff1bMO	43.8	23.2	18.7	14.3	315	6
	sff1bMO	88.2	6.1	3.6	2.1	280	1
	ff1b4MMO	97.6	0.3	1.5	0.6	335	1

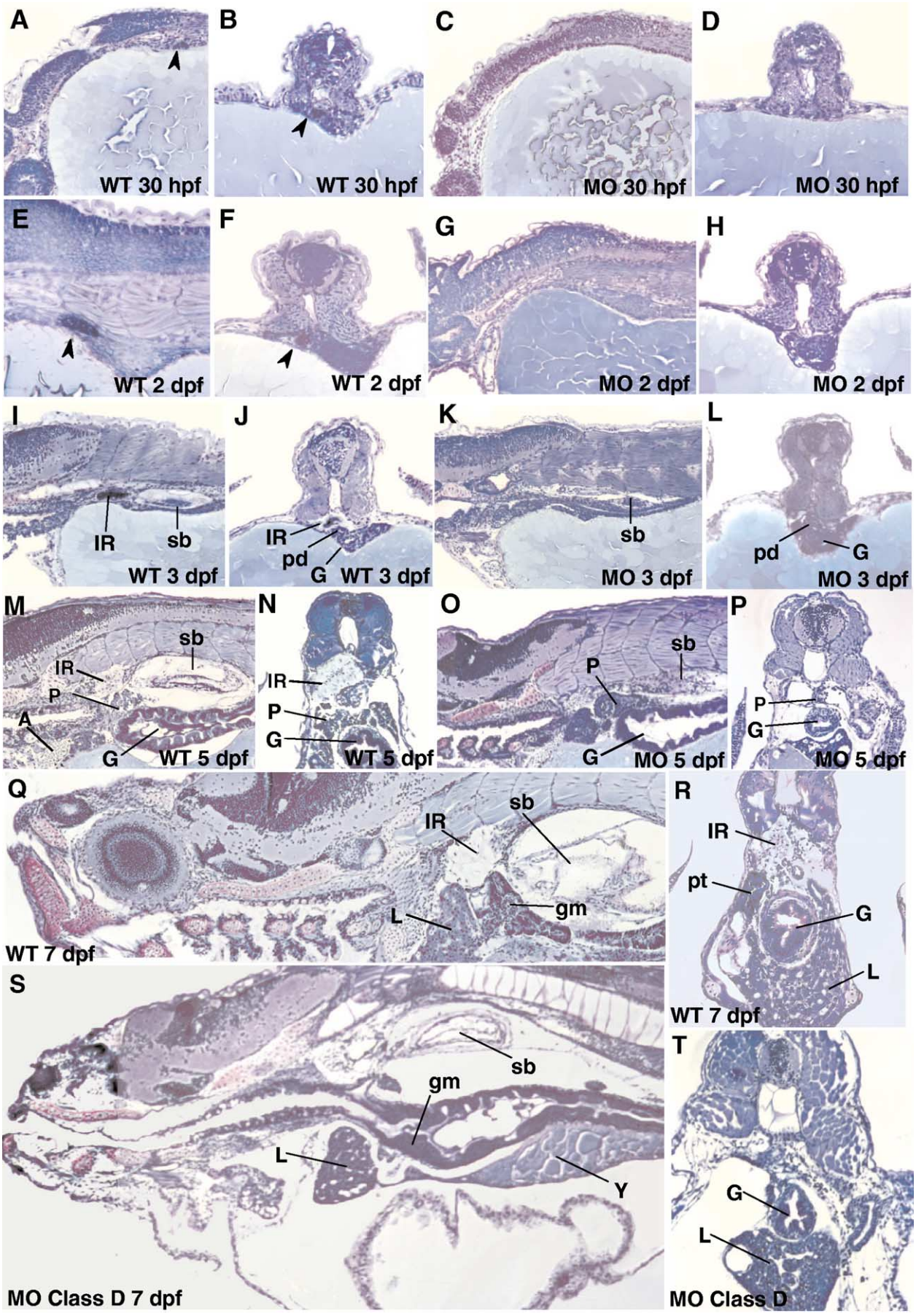
A
WT 30 hpf
B
WT 30 hpf
C
MO 30 hpf
D
MO 30 hpf
E
WT 2 dpf
F
WT 2 dpf
G
MO 2 dpf
H
MO 2 dpf
I
IR
sb
WT 3 dpf
J
IR
pd
G
WT 3 dpf
K
sb
MO 3 dpf
L
pd
G
MO 3 dpf
M
sb
IR
P
A
G
WT 5 dpf
N
IR
P
G
WT 5 dpf
O
sb
P
G
MO 5 dpf
P
P
G
MO 5 dpf
Q
IR
sb
L
gm
WT 7 dpf
R
IR
pt
G
L
WT 7 dpf
S
sb
gm
L
Y
MO Class D 7 dpf
T
G
L
MO Class D

midline and could be seen in transverse section (Fig. 9R). The histopathology of ff1bMO-injected (Class D) embryos at 7 dpf is presented in Fig. 9S and T. In ff1bMO-injected larvae showing apparent wild-type phenotype (Class A), the complete absence of interrenal gland could be noted (data not shown). Myosomial edema was visible in severely affected larvae, resulting in gaps between myofibrils (Fig. 9T). In Class D morphants, the swim bladder was collapsed and reduced in size compared with Class A morphants or wild-type larvae. Failure of the swim bladder to inflate could be due presumably to the build up of turgor pressure in the abdominal cavity as a result of fluid accumulation.

Discussion

In the present study, we have provided several lines of evidence to support a role for *ff1b* in the development of the interrenal organ in the zebrafish. Expression of *ff1b* in the interrenal primordia could be detected at around 27 hpf, appearing initially as bilateral clusters that later coalesce into a single cluster slightly to the right of the midline. At the time when *ff1b* transcripts could be detected, convergence of the clusters is almost complete. Shortly after their coalescence, these cells acquire a steroidogenic phenotype, as shown by their expression of transcripts for the steroidogenic enzyme genes, *3β-hsd* and *cyp11a*. That these cells are capable of producing C_{18} steroids was confirmed by the demonstration of 3β-Hsd enzymatic activity in the presence of its substrate, dehydroepiandrostenedione. Following coalescence of the bilateral clusters, the interrenal of the zebrafish remains as a discrete structure up to 3 dpf, when it begins to display some degree of morphological elaboration.

Convergence of the two *ff1b*-positive cell clusters at the midline is arrested in oep^{m134}, sqt^{c235}, and ntl^{tc41} mutant embryos, resulting in bilateral clusters, while in flh^{tk241} and cyc^{b16} (Chai and Chan, 2000) mutants, the convergence is unperturbed. The expression of *3β-hsd* and *cyp11a* appears to be normal at these ectopic locations, indicating that the steroidogenic cells can develop autonomously. Despite the apparent normal development of interrenal cells at these ectopic locations in mutants, it is likely that, besides Ff1b, additional factors are required for their differentiation at these locations as overexpression of *ff1b* alone in microinjected embryos was not sufficient to induce a steroidogenic fate at other locations (data not shown). This contrasts with mouse SF-1, which when stably expressed in embryonic stem (ES) cells is sufficient to direct them toward a steroidogenic lineage (Crawford et al., 1997). Expression of *cyp11a* and progesterone production in the converted cells could be induced by cotreatment with cAMP and retinoid acid, which are intracellular transducers of SF-1 activity. However, these cells were not responsive to ACTH and hCG, hormones which induce steroidogenesis in adrenal and gonadal cells, respectively, indicating that the receptors for these hormones are probably not expressed in these cells (Crawford et al., 1997). The conversion of the mouse ES cells to steroidogenic lineage therefore appears to be incomplete. SF-1 may require upstream and downstream events to direct the complete differentiation of ES cells, a prerequisite that most likely exists during in vivo steroidogenic cell differentiation.

There is evidence to suggest that one of the accessory factors required for adrenal development is WT-1. WT-1, an obligatory regulator of urogenital development, was shown to be required for adrenal development (Moore et al., 1999). This finding was surprising given that *WT1* is not expressed in the adrenal primordium but only in the earliest adrenogonadal progenitor. Disruption of the *Wt1* locus in mouse abolished adrenal development, a defect that could be partially rescued by introducing a human *WT1* YAC under its native regulatory control (Moore et al., 1999). As in the mouse, *wt1* is not expressed in the interrenal primordium of the zebrafish. It remains a distinct possibility, however, that *wt1*-expressing pronephric cells secrete a diffusible molecule that impacts upon interrenal development and survival in a paracrine fashion. In both oep^{m134} and sqt^{c235} mutants, interrenal and *wt1*-expressing pronephric cells remain in tight association with each other, as in wild-type embryos. This may explain the apparent normal viability of the interrenal cells despite their impaired migration. Such a possibility can be addressed by analyzing interrenal development in zebrafish pronephric mutants or by interfering with *wt1* gene activity using morpholino gene knockdown approach.

Our data show that interrenal cells of the zebrafish arise from bilateral origins in the lateral mesoderm and migrate medially to form a transiently discrete structure, which disperse subsequently to form a diffused organ. Analysis performed in zebrafish midline mutants supports the notion of a mesodermal origin for the interrenal. The failure of *ff1b*-expressing interrenal precursor cells to converge at the midline in oep^{m134} and sqt^{c235}, but not in cyc^{b12}, ntl^{tc41}, and flh^{tk241} mutant embryos, may be explained by impaired convergent-extension of the dorsal mesoderm in these mutants. Convergent-extension involves many different molecules and is important for formation and positioning of tissues along the trunk and tail midline. During the process,

Fig. 9. Histological analysis of the interrenal in wild-type and ff1bMO-injected embryos from 30 hpf to 5 dpf following 3β-Hsd chromogenic staining. Sagittal (A, C, E, G, I, K, M, O, Q, S) and transverse (B, D, F, H, J, L, N, P, R, T) plastic sections of wild-type (A, B, E, F, I, J, M, N, Q, R) and *ff1b* morphant (C, D, I, J, M, N, S, T) embryos at the indicated stages of development. Arrowheads in (A, B, E, and F) indicate the position of the interrenal. Abbreviations: A, atrium; gm, glomerulus; G, gut; IR, interrenal gland; L, liver; MO, morphant; p, pronephros; pd, pneumatic duct; pt, pronephric tubule; sb, swim bladder; WT, wild-type; Y, yolk.

cells within several layers of the mesoderm elongate, exert traction on each other, and intercalate around the midline. This leads to the compaction of the sheets of cells perpendicular to the midline as well as extension of the mesoderm in an anterior–posterior direction. Impaired migration of interrenal precursor cells in these mutants would be consistent with a mesodermal origin as these mutants are known to be defective in convergent-extension movements of mesodermal tissue (Schier et al., 1997; Feldman et al., 2000). Convergent-extension defects have been implicated in the failure of heart tube fusion in *oep* mutant embryos resulting in *cardia bifida* (Reiter et al., 2001). Furthermore, close apposition between the interrenal and pronephric tissue from early stages of development suggests that they may arise from the same germ layer.

A role for *ff1b* in interrenal development and function was demonstrated by morpholino mediated knockdown of *ff1b* activity *in vivo*. Disruption of *ff1b* function during embryogenesis leads to the absence of any overt signs of interrenal development, as evaluated by the expression of steroidogenic markers as well as by histological analysis. Injection of the ff1b morpholino, ff1bMO, clearly abolishes the expression of the steroidogenic enzyme genes *cyp11a* and *3β-hsd* in the interrenal organ. Histological analyses of *ff1b* morphants reveal the lack of interrenal tissue, thus indicating that the observed absence of *cyp11a* and *3β-hsd* expression is most likely due to the loss of structural components of the interrenal tissue. This is supported by the observation that *ff1b* morpholino injection results in the obliteration of a subpopulation of *ff1b*-expressing cells in the interrenal, which most likely represents the steroidogenic compartment. A subpopulation of *ff1b*-positive cells, presumably those at the periphery of the interrenal that do not express steroidogenic enzyme genes, remain unaffected by morpholino injection. However, the identity of these cells remains to be established.

As the interrenal is already at a relatively advanced stage of development by the time steroidogenic markers can be detected or when it becomes histologically distinguishable, it is not possible to conclude from this study whether interrenal development has been affected during early tissue specification or during subsequent organogenesis. In mice, knockout studies have shown that adrenocortical development is initiated in the absence of SF-1 but is not maintained during subsequent development indicating that SF-1 is somehow required for tissue growth and survival (Luo et al., 1994; Sadovsky et al., 1995). However, the mechanisms by which SF-1 exert its effects on these processes remains unknown. It has been proposed that SF-1 may regulate the expression of genes that determine cell proliferation and apoptosis (Parker and Schimmer, 2001).

The phenotypes of larvae resulting from the disruption of *ff1b* functions *in vivo* are consistent with impaired osmoregulatory functions. Edema in various body compartments of *ff1b* morphants indicates a dysfunction in ionic regulation and the failure of the pronephros to excrete excess water. In teleosts, the interrenal plays a central role in osmoregulation by secreting corticosteroids, principally cortisol (Wendelaar Bonga, 1997). Cortisol has been classically regarded as a seawater-adapting hormone (Balment et al., 1987; Henderson and Kime, 1987; Evans, 1993) but more recent evidence has also suggested it to be important for osmoregulation in freshwater fishes (Lin and Randall, 1993; Uchida et al., 1998).

A direct role for the interrenal in osmoregulation in freshwater teleosts has been demonstrated in early studies by using surgical interrenalectomy. In freshwater silver eels, interrenalectomy resulted in a weight gain of 1% per day reflecting net water retention (Chan et al., 1967). The main target sites for cortisol action in the gills of freshwater fishes are the chloride and pavement cells (Kültz and Jürss 1993; Sullivan et al., 1995). While these primary sites for cortisol action are involved mainly in mineral balance, cortisol also acts on sites that are directly involved in regulating water uptake, such as the nephric tubules. Due to their hyperosmotic serum, freshwater fishes tend to gain water passively across permeable surfaces such as the epithelial linings of the gills and gut. To overcome this, they excrete excess water by producing copious amounts of hypotonic urine. Therefore, it is likely that edema phenotype observed for *ff1b* morphant larvae is caused by reduced glomerular filtration rate resulting from the loss of interrenal cortisol production.

Targeted knockout of *SF-1* in mice leads to perinatal lethality within 48 h of birth due to severe adrenocortical insufficiency. *SF-1* knockout pups lack adrenals and exhibit diminished levels of serum corticosterone, accompanied by elevated levels of ACTH as a result of feedback regulation (Sadovsky et al., 1995; Luo et al., 1995). However, zebrafish larvae (Class C and D morphants) lacking overt interrenal development and displaying severe osmoregulatory defects following knockdown of *ff1b* function can survive up to 15 dpf. This indicates a major interspecies difference in the requirement for early adrenocortical functions. In mammals, postnatal functions of the adrenal glands are important for the maintenance of many essential physiological processes, including fluid and mineral balance, energy metabolism, and the immune response. SF-1 knockout mice display volume depletion within 12 h of birth and begin to die (Luo et al., 1995). Lethality in the early stages at least is likely due to the failure to regulate electrolyte and fluid balance.

Some teleosts, however, appear to tolerate considerable fluctuations in serum osmotic concentrations. Fresh water-adapted eels, for instance, can survive up to ~19% reduction in plasma sodium concentration following interrenalectomy (Chan et al., 1969). This may account for the survival of *ff1b* morphant larvae despite severe fluid accumulation in the body. The osmoregulatory phenotypes of *ff1b* knockdown can be mimicked by treatment with the adrenostatic drug, aminoglutethimide, supporting the conclusion that the inhibition of *de novo* steroid synthesis is responsible for the

observed phenotypes. However, while inhibitor treatment has demonstrated a higher penetrance in inducing phenotype, morpholino injection has produced more severe phenotypes at the upper end of its spectrum of effects. This suggests that other pathways of osmoregulation that are not dependent on steroid synthesis had been affected by knockdown of *ff1b*.

It is possible that the delay in yolk absorption in *ff1b* morphants is caused by the lack of interrenal cortisol stimulation of both proteolytic and lipolytic activities necessary for yolk mobilization. As in mammals, cortisol exerts a general catabolic effect in teleosts. The proteolytic action of cortisol has been implicated especially on white muscle and liver, although this has been based mainly on indirect observations of increase in plasma levels of amino acids and proteins following treatment with cortisol or its agonists (Barton et al., 1987; Vijayan et al., 1997). Other evidence comes from correlative observations of the effects of conditions that cause changes in plasma cortisol levels, such as starvation (Storer, 1967; Pickford et al., 1970; Woo and Cheung, 1980), or natural stress, such as spawning migration (McBride et al., 1986) on white muscle proteolysis. In addition to its proteolytic role, cortisol has also been shown to stimulate lipolysis in teleosts (Dave et al., 1979; Lidman et al., 1979; Sheridan, 1986).

Knockdown of *ff1b* function impaired interrenal development in the zebrafish, in a manner analogous to the effect of SF-1 gene disruption on adrenal development in mammals. This indicates a conserved developmental program for the adrenocortical tissue across great evolutionary distances. Accordingly, the loss-of-function phenotypes of *ff1b* can be correlated with the loss of interrenal steroid output, particularly that of cortisol. However, the adrenocorticosteroids do not appear to be absolutely required for maintaining viability during embryonic and larval development. This contrasts sharply with mammals and highlights interspecific differences in corticosteroid requirements. Alternatively, it may reflect different physiological demands between these organisms owing to their drastically different habitats. The postulation that osmoregulatory phenotypes in *ff1b* morphants are due to deficiency in interrenal steroid production is supported by the observation that an inhibitor of steroid synthesis can mimic the phenotypes in treated wild-type embryos. However, the greater severity of defects observed in *ff1b* knockdown compared with inhibitor treatment suggests that *ff1b* may be involved in other mechanisms of osmoregulation that do not involve steroid hormones. One possible mechanism may operate through the action of prolactin, but this needs to be substantiated by experimental evidence.

Acknowledgments

We thank Ms. S.P. Tan for technical assistance. We are also grateful to Assoc. Prof. Vladimir Korzh for the *dβh* cDNA probe, and Prof. Chung Bon-chu for the *3β-hsd* cDNA probe and the sharing of unpublished data. This work was supported by the Institute of Molecular Agrobiology, and National University of Singapore (RP R-154-000-076-112).

References

Balment, R.J., Henderson, I.W., Jones, I.C., 1980. The adrenal cortex and its homologues in vertebrates; evolutionary considerations, in: Jones Henderson, I.W. (Ed.), General, Comparative and Clinical Endocrinology of the Adrenal Cortex, Vol. 3, Academic Press, London, IC, pp. 525–557.

Barton, B.A., Schreck, C.B., Barton, L.D., 1987. Effects of chronic cortisol administration and daily acute stress on growth, physiological conditions, and stress responses in juvenile rainbow trout. Dis. Aquat. Org. 2, 173–185.

Bornstein, S.R., Ehrhart-Bornstein, M., Scherbaum, W.A., Pfeiffer, E.F., Holst, J.J., 1990. Effects of splanchnic nerve stimulation on the adrenal cortex may be mediated by chromaffin cells in a paracrine manner. Endocrinology 127, 900–906.

Bornstein, S.R., Tian, H., Haidan, A., Bottner, A., Hiroi, N., Eisenhofer, G., McCann, S.M., Chrousos, G.P., Roffler-Tarlov, S., 2000. Deletion of tyrosine hydroxylase gene reveals functional interdependence of adrenocortical and chromaffin cell system *in vivo*. Proc. Natl. Acad. Sci. USA 97, 14742–14747.

Bourne, A., 1991. Androgens, in: Pang, P.K.T., Schreibman, M.P. (Eds.), Vertebrate Endocrinology: Fundamentals and Biomedical Implications, Vol. 2, Academic Press, New York, pp. 115–147.

Brand, M., Heisenberg, C.P., Warga, R.M., Pelegri, F., Karlstrom, R.O., Beuchle, D., Picker, A., Jiang, Y.J., Furutani-Seiki, M., van Eeden, F.J., Granato, M., Haffter, P., Hammerschmidt, M., Kane, D.A., Kelsh, R.N., Mullins, M.C., Odenthal, J., Nusslein-Volhard, C., 1996. Mutations affecting development of the midline and general body shape during zebrafish embryogenesis. Development 123, 129–142.

Carroll, T.J., Vize, P.D., 1996. Wilms' tumor suppressor gene is involved in the development of disparate kidney forms: evidence from expression in the *Xenopus* pronephros. Dev. Dyn. 206, 131–138.

Chai, C., Chan, W.K., 2000. Developmental expression of a novel *Ftz-F1* homologue, *ff1b (NR5A4)*, in the zebrafish *Danio rerio*. Mech. Dev. 91, 421–426.

Chan, D.K., Jones, I.C., Henderson, I.W., Rankin, J.C., 1967. Studies on the experimental alteration of water and electrolyte composition of the eel (*Anguilla anguilla* L.). J. Endocrinol. 37, 297–317.

Chan, D.K.O., Rankin, J.C., Jones, I.C., 1969. Influences of the adrenal cortex and the corpuscles of Stannius on osmoregulation in the European eel (*Anguilla anguilla L.*) adapted to freshwater. Gen. Comp. Endocr. Suppl. 2, 342–353.

Conlon, F.L., Lyons, K.M., Takaesu, N., Barth, K.S., Kispert, A., Herrmann, B., Robertson, E.J., 1994. A primary requirement for nodal in the formation and maintenance of the primitive streak in the mouse. Development 120, 1919–1928.

Contreras, H., Ronco, A.M., 1994. Leydig cell heterogencity as judged by quantitative cytochemistry of 3 beta-hydroxysteroid dehydrogenase activity in individual rat Leydig cells. J. Steroid Biochem. Mol. Biol. 51, 73–79.

Crawford, P.A., Sadovsky, Y., Milbrandt, J., 1997. Nuclear receptor steroidogenic factor 1 directs embryonic stem cells toward the steroidogenic lineage. Mol. Cell. Biol. 17, 3997–4006.

Dave, G., Johannsson-Sjöbeck, M.-L., Larsson, ÅA., Lewander, K., Lidman, U., 1979. Effects of cortisol on the fatty acid composition of the total blood plasma lipids in the European eel, *Anguilla anguilla*. L. Comp. Biochem. Physiol. 64A, 37–40.

DeLean, A., Raca, K., McNicoll, N., Desrosiers, M.L., 1984. Direct β-adrenergic stimulation of aldosterone secretion in cultured bovine adrenal subcapsular cells. Endocrinology 115, 485–492.

Dodd, J., Jessell, T.M., Placzek, M., 1998. The when and where of floor plate induction. Science 282 (5394), 1654–1657.

Drummond, I.A., Majumdar, A., Hentschel, H., Elger, M., Solnica-Krezel, L., Schier, A.F., Neuhauss, S.C., Stemple, D.L., Zwartkruis, F., Rangini, Z., Driever, W., Fishman, M.C., 1998. Early development of the zebrafish pronephros and analysis of mutations affecting pronephric function. Development 125, 4655–4667.

Ehrhart-Bornstein, M., Bornstein, S.R., Gonzalez-Hernandez, J., Holst, J.J., Waterman, M.R., Scherbaum, W.A., 1995. Sympathoadrenal regulation of adrenocortical steroidogenesis. Endocr. Res. 21, 13–24.

Ekker, S.C., 2000. Morphants: a new systematic vertebrate functional genomics approach. Yeast 17, 302–306.

Evans, D.H., 1993. Osmotic and ionic regulation, in: Evans, D.H. (Ed.), The Physiology of Fishes, CRC Press, Boca Raton, pp. 315–341.

Feldman, B., Gates, M.A., Egan, E.S., Dougan, S.T., Rennebeck, G., Sirotkin, H.I., Schier, A.F., Talbot, W.S., 1998. Zebrafish organizer development and germ-layer formation require nodal-related signals. Nature 395, 181–185.

Feldman, B., Dougan, S.T., Schier, A.F., Talbot, W.S., 2000. Nodal-related signals establish mesendodermal fate and trunk neural identity in zebrafish. Curr. Biol. 4, 531–534.

Gallo, V.P., Civinini, A., Mastrolia, L., Leitner, G., Porta, S., 1993. Cytological and biochemical studies on chromaffin cells in the head kidney of *Gasterosteus aculeatus* (Teleostei, Gasterosteidae). Gen. Comp. Endocrinol. 92, 133–142.

Gfell, B., Kloas, W., Hanke, W., 1997. Neuroendocrine effects on adrenal hormone secretion in carp (*Cyprinus carpio*). Gen. Comp. Endocrinol. 106, 310–309.

Giacomini, E., 1934. Ulterori ricerche anatomomicroscopiche ed organogenetiche sul sistema interrenale e sui corpuscoli di Stan-nius dei Teleostei e dei Ganoidi. Rend. R. Acad. Sci. Ist. Bologna 38, 127–140.

Glasgow, E., Tomarev, S.I., 1998. Restricted expression of the homeobox gene prox 1 in developing zebrafish. Mech. Dev. 76, 175–178.

Grassi Milano, E., Basari, F., Chimenti, C., 1997. Adrenocortical and adrenomedullary homologs in eight species of adult and developing teleosts: morphology, histology, and immunohistochemistry. Gen. Comp. Endocrinol. 108, 483–496.

Graves, P.E., Salhanick, H.A., 1979. Stereoselective inhibition of aromatase by enantiomers of aminoglutethimide. Endocrinology 105, 52–57.

Haidan, A., Bornstein, S.R., Glasow, A., Uhlmann, K., Lubke, C., Ehrhart-Bornstein, M., 1998. Basal steroidogenic activity of adrenocortical cells is increased 10-fold by coculture with chromaffin cells. Endocrinology 139, 772–780.

Halpern, M.E., Ho, R.K., Walker, C., Kimmel, C.B., 1993. Induction of muscle pioneers and floor plate is distinguished by the zebrafish no tail mutation. Cell 75, 99–111.

Hanke, W., Kloas, W., 1995. Comparative aspects of regulation and function of the adrenal complex in different groups of vertebrates. Horm. Metab. Res. 27, 389–397.

Hardisty, M.W., 1972. The Biology of Lampreys, Hardisty, M.W., Potter, I.C. (Eds.), Vol. 2, Academic Press, London.

Hartman, F.A., Brownell, K.A., 1949. The Adrenal Gland. Henry Kimpton, London.

Hathaway, C.B., Epple, A., 1990. Catecholamines, opioid peptides, and true opiates in the chromaffin cells of the eel: immunohistochemical evidence. Gen. Comp. Endocrinol. 79, 393–405.

Hatta, K., Kimmel, C.B., Ho, R.K., Walker, C., 1991. The cyclops mutation blocks specification of the floor plate of the zebrafish central nervous system. Nature 350, 339–441.

Heller, N., Brandli, A.W., 1997. Xenopus Pax-2 displays multiple splice forms during embryogenesis and pronephric kidney development. Mech. Dev. 69, 83–104.

Henderson, I.W., Kime, D.E., 1987. The adrenal cortical steroids, in: Pang, P.K.T., Schreibman, M.P. (Eds.), Vertebrate Endocrinology: Fundamentals and Biomedical Implications, Vol. 2, Academic Press, New York, pp. 121–142.

Holmes, W.N., Phillips, J.G., 1976. In: General and Comparative and Clinical Endocrinology of the Adrenal Cortex, Jones, I.C., Henderson, I.W. (Eds.), Vol. 1, Academic Press, London, pp. 293–420.

Idelman, I., 1978. In: General and Comparative and Clinical Endocrinology of the Adrenal Cortex, Jones, I.C., Henderson, I.W. (Eds.), Vol. 2, Academic Press, London, pp. 1–200.

Jones, I.C., Mosley, W., 1980. The interrenal gland in Pisces, in: Jones, I.C., Henderson, I.W. (Eds.), General, Comparative and Clinical Endocrinology of the Adrenal Cortex, Vol. 3, Academic Press, San Francisco, pp. 395–472.

Karlstrom, R.O., Trowe, T., Klostermann, S., Baier, H., Brand, M., Crawford, A.D., Grunewald, B., Haffter, P., Hoffmann, H., Meyer, S.U., Muller, B.K., Richter, S., van Eeden, F.J., Nusslein-Volhard, C., Bonhoeffer, F., 1996. Zebrafish mutations affecting retinotectal axon pathfinding. Development 123, 427–438.

Kimmel, C.B., Ballard, W.W., Kimmer, S.R., Ullmann, B., Schilling, T.F., 1995. Stages of embryonic development of the zebrafish. Dev. Dyn. 203, 253–310.

Kodjabachian, L., Dawid, I.B., Toyama, R., 1999. Gastrulation in zebrafish: what mutants teach us. Dev. Biol. 213, 231–245.

Kreidberg, J.A., Sariola, H., Loring, J.M., Maeda, M., Pelletier, J., Housman, D., Jaenisch, R., 1993. WT-1 is required for early kidney development. Cell 74, 679–691.

Kültz, D., Jürss, K., 1993. Biochemical characterization of isolated branchial mitochondria-rich cells of *Oreochromis mossambicus* acclimated to fresh water or hyperhaline sea water. J. Comp. Physiol. B 163, 406–412.

Lai, W.W., Hsiao, P.H., Guiguen, Y., Chung, B.C., 1998. Cloning of zebrafish cDNA for 3beta-hydroxysteroid dehydrogenase and P450scc. Endocr. Res. 24, 927–931.

Lidman, U., Dave, G., Johansson-Sjöbeck, M.-L., Larsson, ÅA., Lewander, K., 1979. Metabolic effects of cortisol in the European eel, *Anguilla anguilla* (LeSueur). Comp. Biochem. Physiol. 63B, 339–344.

Lin, H., Randall, D.J., 1993. Proton-ATPase activity in crude homogenates of fish gill tissue: inhibitor sensitivity and environmental and hormonal regulation. J. Exp. Biol. 180, 163–174.

Liu, Y.W., Chan, W.K., 2002. Thyroid hormones are important for embryonic to larval transitory phase in zebrafish. Differentiation 70, 36–45.

Lofts, B., 1978. In: General and Comparative and Clinical Endocrinology of the Adrenal Cortex, Jones, I.C., Henderson I.W. (Eds.), Vol. 2, Part I, Academic Press, London, pp. 292–369.

Luo, X., Ikeda, Y., Parker, K.L., 1994. A cell-specific nuclear receptor is essential for adrenal and gonadal development and sexual differentiation. Cell 77, 481–490.

Luo, X., Ikeda, Y., Schlosser, D.A., Parker, K.L., 1995. Steroidogenic factor 1 is the essential transcript of the mouse *Ftz-F1* gene. Mol. Endocrinol. 9, 1233–1239.

McBride, J.R., Fagerlund, U.H.M., Dye, H.M., Bagshaw, J., 1986. Changes in structure of tissues and in plasma cortisol during the spawning migration of pink salmon (*Oncorhynchus gorbuscha* (Walbaum)). J. Fish Biol. 29, 153–166.

Moore, A.W., McInnes, L., Kreidberg, J., Hastie, N.D., Schedl, A., 1999. YAC complementation shows a requirement for Wt1 in the development of epicardium, adrenal gland and throughout nephrogenesis. Development 126, 1845–1857.

Nandi, J., 1962. The structure of the interrenal gland in teleost fishes. Univ. Calif. Publ. Zool. 65, 129–212.

Nachtigal, M.W., Hirokawa, Y., Enyeart-VanHouten, D.L., Flanagan, J.N., Hammer, G.D., Ingraham, H.A., 1998. Wilms' tumor 1 and Dax-1 modulate the orphan nuclear receptor SF-1 in sex-specific gene expression. Cell 93, 445–454.

Nasevicius, A., Ekker, S.C., 2000. Effective targeted gene "knockdown" in zebrafish. Nat. Genet. 26, 216–220.

Odenthal, J., Haffter, P., Vogelsang, E., Brand, M., van Eeden, F.J., Furutani-Seiki, M., Granato, M., Hammerschmidt, M., Heisenberg, C.P., Jiang, Y.J., Kane, D.A., Kelsh, R.N., Mullins, M.C., Warga, R.M., Allende, M.L., Weinberg, E.S., Nusslein-Volhard, C., 1996. Mutations affecting the formation of the notochord in the zebrafish, *Danio rerio*. Development 123, 103–115.

Parker, K.L., Schimmer, B.P., 2001. Genetics of the development and function of the adrenal cortex. Rev. Endocr. Metab. Disord. 2, 245–252.

Pickford, G.E., Pang, P.K.T., Weinstein, E., Toretti, J., Hendler, E., Epstein, F.H., 1970. The response of the hypothysectomized cyprinodont, *Fundulus heteroclitus*, to replacement therapy with cortisol: effects on blood serum and sodium-potassium activated adenosine triphosphatase in the gills, kidney, and intestinal mucosa. Gen. Comp. Endocrinol. 14, 524–534.

Pratt, H.J., Turner, A.D., McAteer, A.J., Henry, P.D., 1985. β-Adrenergic stimulation of aldosterone production by rat adrenal capsular explants. Endocrinology 117, 1189–1194.

Rebagliati, M.R., Toyama, R., Haffter, P., Dawid, I.B., 1998. cyclops encodes a nodal-related factor involved in midline signaling. Proc. Natl. Acad. Sci USA 95, 9932–9997.

Reid, S.G., Fritsche, R., Jonsson, A.C., 1995. Immunohistochemical localization of bioactive peptides and amines associated with the chromaffin tissue of five species of fish. Cell Tissue Res. 280, 499–512.

Reid, S.G., Vijayan, M.M., Perry, S.F., 1996. Modulation of catecholamine storage and release by the pituitary-interrenal axis in the rainbow trout, *Oncorhynchus mykiss*. J. Comp. Physiol. B 165, 665–676.

Reiter, J.F., Verkade, H., Stainier, D.Y., 2001. Bmp2b and Oep promote early myocardial differentiation through their regulation of gata5. Dev. Biol. 234, 330–338.

Rodriguez-Niedenfuhr, M., Papoutsi, M., Christ, B., Nicolaides, K.H., von Kaisenberg, C.S., Tomarev, S.I., Wilting, J., 2001. Prox1 is a marker of ectodermal placodes, endodermal compartments, lymphatic endothelium and lymphangioblasts. Anat. Embryol. (Berl.) 204, 399–406.

Sadovsky, Y., Crawford, P.A., Woodson, K.G., Polish, J.A., Clements, M.A., Tourtellotte, L.M., Simburger, K., Milbrandt, J., 1995. Mice deficient in the orphan receptor steroidogenic factor 1 lack adrenal glands and gonads but express P450 side-chain-cleavage enzyme in the placenta and have normal embryonic serum levels of corticosteroids. Proc. Natl. Acad. Sci USA 92, 10939–10943.

Sampath, K., Rubinstein, A.L., Cheng, A.M., Liang, J.O., Fekany, K., Solnica-Krezel, L., Korzh, V., Halpern, M.E., Wright, C.V., 1998. Induction of the zebrafish ventral brain and floorplate requires cyclops/nodal signalling. Nature 395, 185–189.

Schier, A., Neuhauss, S.C., Helde, K.A., Talbot, W.S., Driever, W., 1997. The one-eyed pinhead gene functions in mesodem and endoderm formation in zebrafish and interacts with no-tail. Development 124, 327–342.

Schulte-Merker, S., Ho, R.K., Herrmann, B.G., Nusslein-Volhard, C., 1992. The protein product of the zebrafish homologue of the mouse T gene is expressed in nuclei of the germ ring and the notochord of the early embryo. Development 116, 1021–1032.

Schulte-Merker, S., van Eeden, F.J., Halpern, M.E., Kimmel, C.B., Nusslein-Volhard, C., 1994. *no tail (ntl)* is the zebrafish homologue of the mouse T (*Brachyury*) gene. Development 120, 1009–1015.

Semba, K., Saito-Ueno, R., Takayama, G., Kondo, M., 1996. cDNA cloning and its pronephros-specific expression of the Wilms' tumor suppressor gene, *WT1*, from *Xenopus laevis*. Gene 175, 167–172.

Selcer, K.W., Leavitt, W.W., 1991. Estrogens and progestins, in: Pang, P.K.T., Schreibman, M.P. (Eds.), Vertebrate Endocrinology: Fundamentals and Biomedical Implications, Academic Press, New York, pp. 67–114.

Shepherd, S.P., Holzwarth, M.A., 2001. Chromaffin-adrenocortical cell interactions: effects of chromaffin cell activation in adrenal cell cocultures. Am. J. Physiol. Cell. Physiol. 280, C61–C71.

Sheridan, M.A., 1986. Effects of thyroxin, cortisol, growth hormone and prolactin on lipid metabolism of coho salmon, *Oncorhynchus kisutch*, during smoltification. Gen. Comp. Endocrinol. 64, 220–238.

Shinoda, K., Lei, H., Yoshii, H., Nomura, M., Nagano, M., Shiba, H., Sasaki, H., Osawa, Y., Ninomiya, Y., Niwa, O., Morohashi, K.-I., Li, E., 1995. Developmental defects of the ventromedial hypothalamic nucleus and pituitary gonadotroph in the Ftz-F1 disrupted mice. Dev. Dyn. 204, 22–29.

Storer, G.H., 1967. Starvation and the effects of cortisol in the goldfish (*Carassius auratus*). Comp. Biochem. Physiol. 20, 939–948.

Strahle, U., Jesuthasan, S., Blader, P., Garcia-Villalba, P., Hatta, K., Ingham, P.W., 1997. *one-eyed pinhead* is required for development of the ventral midline of the zebrafish (*Danio rerio*) neural tube. Genes Funct. 1, 131–148.

Sullivan, G., Fryer, J., Perry, S., 1995. Immunolocalization of proton pumps (H + ATPase) in pavement cells of rainbow trout gill. J. Exp. Biol. 198, 2619–2629.

Thompson Jr., E.A., Siiteri, P.K., 1974. The involvement of human placental microsomal cytochrome P-450 in aromatization. J. Biol. Chem. 249, 5373–5378.

Torres, M., Gornez-Pardo, E., Dressler, G.R., Gruss, P., 1995. Pax-2 controls multiple steps of urogenital development. Development 121, 4057–4065.

Uchida, K., Kaneko, T., Tagawa, M., Hirano, T., 1998. Localization of cortisol receptor in branchial chloride cells in chum salmon fry. Gen. Comp. Endocrinol. 109, 175–185.

Uzgiris, V.I., Whipple, C.A., Salhanick, H.A., 1977. Stereoselective inhibition of cholesterol side chain cleavage by enantiomers of aminoglutethimide. Endocrinology 101, 89–92.

Vijayan, M.M., Pereira, C., Grau, E.G., Iwama, G.K., 1997. Metabolic responses associated with confinement stress in tilapia: the role of cortisol. Comp. Biochem. Physiol. 116C, 89–95.

Wendelaar Bonga, S.E., 1997. The stress response in fish. Physiol. Rev. 77, 591–625.

Westerfield, M., 2000. The Zebrafish Book: Guide for the Laboratory Use of Zebrafish (*Danio rerio*), 4th Ed. Univ. of Oregon Press, Eugene, OR.

Whipple, C.A., Colton, T., Strauss, J.M., Hourihan, J., Salhanick, H.A., 1978. Comparison of luteolytic potencies of aminoglutethimide enantiomers in the rabbit and rat. Endocrinology 103, 1605–1610.

Wigle, J.T., Oliver, G., 1999. Prox 1 function is required for the development of the murine lymphatic system. Cell 98, 769–778.

Woo, N.Y.S., Cheung, S.I., 1980. Metabolic effects of starvation in the snakehead, *Ophiocephalus maculatus*. Comp. Biochem. Physiol. 67A, 623–627.

Wrobel, K.H., SuB, F., 1999. On the origin and prenatal development of the bovine adrenal gland. Anat. Embryol. (Berl.) 199, 301–318.

Yu, R., Ito, M., Jameson, J.L., 1997. DAX-1 inhibits SF-1-mediated transactivation via a carboxy-terminal domain that is deleted in adrenal hypoplasia congenita. Mol. Cell. Biol. 17 (3), 1476–1483.

Zhang, Y.H., Guo, W., Wagner, R.L., Huang, B.L., McCabe, L., Vilain, E., Burris, T.P., Anyane-Yeboa, K., Burghes, A.H., Chitayat, D., Chudley, A.E., Genel, M., Gertner, J.M., Klingensmith, G.J., Levine, S.N., Nakamoto, J., New, M.I., Pagon, R.A., Pappas, J.G., Quigley, C.A., Rosenthal, I.M., Baxter, J.D., Fletterick, R.J., McCabe, E.R., 1998. DAX1 mutations map to putative structural domains in a deduced three-dimensional model. Am. J. Hum. Genet. 62, 855–864.

Zhou, X., Sasaki, H., Lowe, L., Hogan, B.L., Kuehn, M.R., 1993. Nodal is a novel TGF-beta-like gene expressed in the mouse node during gastrulation. Nature 361, 543–547.